

# **SANDIA REPORT**

SAND2006-2189

Unlimited Release

Printed April 2006

## **A 50-100 kWe Gas-cooled Reactor For Use On Mars**

Curtis D. Peters

Prepared by  
Sandia National Laboratories  
Albuquerque, New Mexico 87185 and Livermore, California 94550

Sandia is a multiprogram laboratory operated by Sandia Corporation,  
a Lockheed Martin Company, for the United States Department of Energy's  
National Nuclear Security Administration under Contract DE-AC04-94AL85000.

Approved for public release; further dissemination unlimited.

Issued by Sandia National Laboratories, operated for the United States Department of Energy by Sandia Corporation.

**NOTICE:** This report was prepared as an account of work sponsored by an agency of the United States Government. Neither the United States Government, nor any agency thereof, nor any of their employees, nor any of their contractors, subcontractors, or their employees, make any warranty, express or implied, or assume any legal liability or responsibility for the accuracy, completeness, or usefulness of any information, apparatus, product, or process disclosed, or represent that its use would not infringe privately owned rights. Reference herein to any specific commercial product, process, or service by trade name, trademark, manufacturer, or otherwise, does not necessarily constitute or imply its endorsement, recommendation, or favoring by the United States Government, any agency thereof, or any of their contractors or subcontractors. The views and opinions expressed herein do not necessarily state or reflect those of the United States Government, any agency thereof, or any of their contractors.

Printed in the United States of America. This report has been reproduced directly from the best available copy.

Available to DOE and DOE contractors from

U.S. Department of Energy  
Office of Scientific and Technical Information  
P.O. Box 62  
Oak Ridge, TN 37831

Telephone: (865) 576-8401  
Facsimile: (865) 576-5728  
E-Mail: [reports@adonis.osti.gov](mailto:reports@adonis.osti.gov)  
Online ordering: <http://www.osti.gov/bridge>

Available to the public from

U.S. Department of Commerce  
National Technical Information Service  
5285 Port Royal Rd.  
Springfield, VA 22161

Telephone: (800) 553-6847  
Facsimile: (703) 605-6900  
E-Mail: [orders@ntis.fedworld.gov](mailto:orders@ntis.fedworld.gov)  
Online order: [http://www.ntis.gov/help/ordermethods.asp?loc=7-4-](http://www.ntis.gov/help/ordermethods.asp?loc=7-4-0#online)

[0#online](#)



# **A 50-100 kWe Gas-cooled Reactor For Use On Mars**

Curtis D. Peters (Year Round Intern)  
Advanced Nuclear Concepts

Sandia National Laboratories  
P.O. Box 5800  
Albuquerque, New Mexico 87185

## **Abstract**

In the space exploration field there is a general consensus that nuclear reactor powered systems will be extremely desirable for future missions to the outer solar system. Solar systems suffer from the decreasing intensity of solar radiation and relatively low power density. Radioisotope Thermoelectric Generators are limited to generating a few kilowatts electric (kWe). Chemical systems are short-lived due to prodigious fuel use. A well designed 50-100 kWe nuclear reactor power system would provide sufficient power for a variety of long term missions. This thesis will present basic work done on a 50-100 kWe reactor power system that has a reasonable lifespan and would function in an extraterrestrial environment. The system will use a Gas-Cooled Reactor that is directly coupled to a Closed Brayton Cycle (GCR-CBC) power system. Also included will be some variations on the primary design and their effects on the characteristics of the primary design. This thesis also presents a variety of neutronics related calculations, an examination of the reactor's thermal characteristics, feasibility for use in an extraterrestrial environment, and the reactor's safety characteristics in several accident scenarios. While there has been past work for space reactors, the challenges introduced by thin atmospheres like those on Mars have rarely been considered.

## **ACKNOWLEDGEMENTS**

The author wishes to thank Ronald J. Lipinski (SNL), Robert Busch (UNM), Steven A. Wright (SNL), Roger X. Lenard (SNL), and Kendall R. DePriest (SNL) for providing technical assistance, opportunity and guidance in the creation of this report.

The author also wishes to thank the Sandia National Laboratories (SNL) Student Internship Program (SIP) for making this report possible.

## TABLE OF CONTENTS

LIST OF FIGURES .....	ix
LIST OF TABLES .....	x
1.0 Problem Description and Scope of Design .....	1
1.1 Problem Description .....	1
1.2 Design Scope .....	3
2.0 Background and Literature Review .....	4
2.1 Gas-Cooled Reactor .....	4
2.1.1 History of Gas-cooled Reactors .....	5
2.1.2 How a Gas-cooled Reactor Works .....	5
2.2 Brayton Cycle .....	6
2.2.1 Brayton Cycle History .....	7
2.2.2 Brayton Cycle: How It Works .....	7
2.3 Fast Spectrum Reactor .....	9
2.4 Fuel .....	10
2.5 Pin Type Geometry .....	11
2.6 Space Environment .....	11
3.0 Materials Used in the Design .....	13
3.1 Uranium Nitride .....	13
3.2 Helium/Xenon .....	17
3.3 Niobium 1% Zirconium .....	18
3.4 Hastelloy X .....	21
3.5 Beryllium Oxide .....	23

3.6	Rhenium.....	25
4.0	Design Description.....	27
4.1	Design of Reactor .....	27
4.2	Gas Flow in Reactor.....	34
4.3	Pressure Vessel Composition.....	35
4.4	Core Block Composition.....	35
4.5	Reactor Control Methods.....	36
5.0	Neutronic Investigation into Core Design Results.....	38
5.1	Initial Calculations.....	38
5.2	Reactor Multiplication Vs Reflector Position.....	39
5.3	High Temperature Feedback effects .....	42
5.4	Accident Scenarios.....	45
	5.4.1 Immersion in Water .....	46
	5.4.2 Immersion in Wet Sand with Water Flooding.....	46
	5.4.3 Dry Sand Burial .....	48
5.5	Alternative Cores .....	50
	5.5.1 Category-III Reactor .....	50
	5.5.1.1 Alternative 1 Reactor .....	52
	5.5.1.2 Alternative 2 Reactor .....	55
	5.5.2 Boron Carbide Central Safety Rod .....	57
5.6	Quality Control Runs .....	62
6.0	Thermal Evaluation of Core and Remainder of System.....	66
6.1	Radiator.....	67

7.0	Conclusions and Future Work .....	72
7.1	Conclusions.....	72
7.2	Future Work.....	73
8.0	References.....	70

## LIST OF FIGURES

Figure 1-1. Regions of applicability for different power systems .....	1
Figure 2-1. Closed Brayton Cycle .....	8
Figure 3-1. UN Phase Diagram .....	14
Figure 3-2. UN Mechanical Properties .....	15
Figure 3-3. UN Thermal Properties .....	16
Figure 3-4. Nb1Zr Operational Domain .....	19
Figure 3-5. Nb1Zr Thermal Properties .....	20
Figure 3-6. Hastelloy X Operational Domain .....	22
Figure 3-7. Hastelloy X Thermal Properties .....	23
Figure 3-8. BeO Mechanical Properties .....	24
Figure 3-9. BeO Thermal Properties .....	25
Figure 4-1. XZ Plane Section of Reactor .....	30
Figure 4-2. XY Plane Section of Reactor .....	31
Figure 4-3. XZ Plane Section of Individual Fuel Pin .....	32
Figure 4-4. XY Plane Section of Fuel Pin .....	33
Figure 4-5. Flow Pattern for Reactor .....	34
Figure 4-6. Reflector Movement .....	36
Figure 4-7. XY Plane Section with Radial Reflectors .....	37
Figure 5-1. k-Effective Vs Reflector Gap .....	40
Figure 5-2. Reflector Movement .....	41
Figure 5-3. Flux Profile Vs Position for 3 different reflector settings .....	42
Figure 5-4. Water Immersion Accident Scenario .....	47
Figure 5-5. Wet Sand, Water Scenario .....	48
Figure 5-6. Sand Burial Accident Scenario .....	49
Figure 5-7. XZ Plane Section of Reactor Alternative 1 .....	52
Figure 5-8. XY Cross Section of Reactor Alternative 1 .....	53
Figure 5-9. Close up of XY plane, Alternative 1 Reactor .....	53
Figure 5-10. k-Effective Vs Pitch, Alternative 1 Core .....	54
Figure 5-11. XZ Cross Section of Alternative 2 Reactor .....	56
Figure 5-12. XY Cross Section of Alternative 2 Reactor .....	56
Figure 5-13. Close up of XY Plane, Alternative 2 Reactor .....	57
Figure 5-14. XY Plane Section of Internal Control Rod Reactor .....	58
Figure 5-15. XZ Plane Section of Internal Control Rod Reactor .....	58
Figure 5-16. Multiplication vs. Run with different RNG seeds .....	63
Figure 5-17. Distribution of Fission Causing Neutrons .....	64
Figure 6-1. FEPSIM components with State temperatures .....	66
Figure 6-2. Electric Output vs. Thermal Output .....	68
Figure 6-3. Conversion Efficiency Vs Thermal Output .....	69
Figure 6-4. Specific Power Vs Thermal Output .....	70

## LIST OF TABLES

Table 3-1 Gas Properties .....	18
Table 4-1 Primary Core Parameters.....	28
Table 5-1 Temperature Profile of Reactor .....	43
Table 5-2 Temperature Adjusted Dimensions of the Reactor .....	43
Table 5-3 Temperature Adjusted Material Densities.....	45
Table 5-4 Accident Scenario Results.....	49
Table 5-5 Reactor Dimensions and Compositions.....	60



# 1 Problem Description and Scope of Design

## 1.1 Problem Description

The need for power sources that can generate more power for longer periods of time for space applications has been understood for quite some time. Solar powered systems are good for low power, intermediate-to-long duration missions. Chemical systems are good for low power, intermediate-to-long duration missions. Chemical systems are ideal for high power, short duration missions. Radioisotope Thermoelectric Generators (RTGs) are good for long duration, low power missions. For long-life, high power applications nuclear reactors seem to be the best option available, as shown in Figure 1-1.

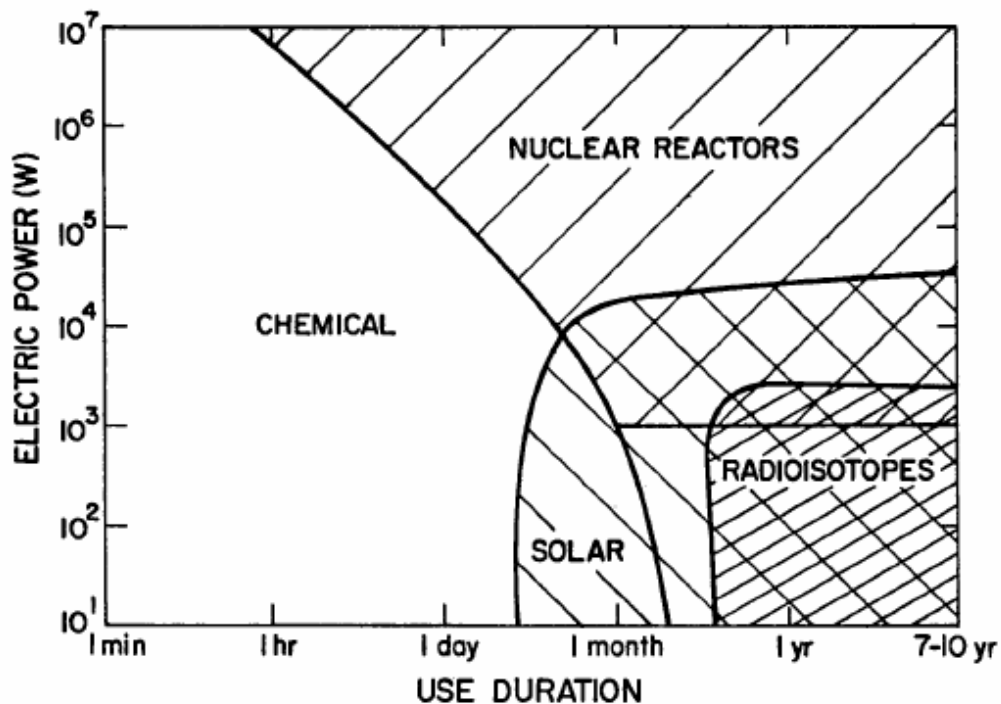


**Figure 1-1. Regions of applicability for different power systems [LA-7858, 1979]**

This plot has a limitation; it is designed for distances from the sun that are comparable to the earth's orbit. At distances further from the sun, the region dominated by solar power

shrinks drastically. There are other considerations; on the moon, which has a 348 hour long night, the solar power regime is also much smaller. This plot shows that for systems requiring more than ten kilowatts of electric power (kWe) for more than a month, nuclear reactors end up being a favorable power source.

Why are systems that generate more power needed? More power means that more science instruments can be fielded, a greater amount of data can be transmitted more quickly, energy intensive applications like electric thrusters become practical, and more complicated missions are possible. Most current probes fly by their target rather than orbit it. Probes that use nuclear powered electric drives can place themselves in a stable orbit around the target and keep examining it. For manned missions, nuclear reactors generate the kind of power required to sustain life and manufacture fuel for return missions. Nuclear reactors are a good method for generating this constant and sustained power.

Currently RTG's are used to produce power for many probes that are transmitting data from across the solar system [Furlong, 1999]. However, RTG's and other systems are limited in power generation because of the limited amount of available  $^{238}\text{Pu}$ , the expense of that isotope, and the fuel needed for a multi-kWe system. The weight per kWe may be unacceptable for some missions. Nuclear fission power systems have the potential to provide more power than RTG's. A drawback of reactor systems is that they are only mass and cost effective for missions requiring more than 10 kWe. Mars and other planets provide another set of potential challenges. The interaction between the outer surfaces of a heated reactor and the atmospheres of these planets is far more complicated than the interaction between the outer surfaces and deep space.

## **1.2 Design Scope**

The goal of this thesis is to present a design for a workable gas-cooled, direct Brayton cycle reactor that could generate 50-100 kWe. The design has not been optimized, but some sensitivity studies were done. The goals were as follow:

- The reactor shall be a gas-cooled, pin type reactor.
- The power output of the reactor will be roughly 100 kWe.
- There shall be reasonable expectation that the reactor can operate at full power for 10 years.
- The reactor will be safe under credible accident scenarios
- Investigate how to modify the reactor so that it is useable in a Martian atmosphere.

For purposes of limiting the scope of the thesis, the reactor will use a directly coupled closed Brayton cycle for power conversion and will use highly enriched Uranium Nitride fuel. The sections of the thesis will be:

- The primary components of a GCR-CBC reactor
- The properties of the materials used in the reactor.
- A description of the reactor core.
- Neutronics related calculations.
- The radiator and how it affects the power conversion section.
- Conclusions and future work.

## 2 Background and Literature Review

This section covers several topics: the history of the important components for the reactor, how these components work, and why these components were chosen. The primary motivation was to design a functional reactor; not to explore all the myriad of possibilities that exist. This meant that not all the alternatives for any given component would be examined, just ones that appeared to fulfill the desired goals. As a result several simplifications were implemented for this thesis to reduce the scope.

The topics that will be examined are:

- What gas-cooled reactors are and how they operate;
- The operation and history of the Brayton Cycle;
- The type of fuel selected.;
- How the fuel is loaded;
- The neutron energy spectrum; and
- The effects of Mars' atmosphere on the exposed components at the expected temperatures.

### 2.1 *Gas-Cooled Reactor*

A gas-cooled nuclear reactor was chosen due to its simplicity and suitability for the space environment. There are numerous alternatives for cooling a reactor core, but gas cooling is one of the simpler methods and most attractive when used with a closed Brayton cycle (CBC) power conversion system. The use of other reactor coolants would necessitate the inclusion of a heat exchanger and introduce complicated freeze/thaw problems, increasing the complexity and the weight of the reactor.

### **2.1.1 History of Gas-cooled Reactors**

Gas-cooled reactors have been around since the early days of the nuclear industry. While none have been flown as space reactors, there is a significant body of work in the form of test reactors and even commercial power reactors. Notable Gas-cooled commercial power reactors include the British MAGNOX reactors, Peach Bottom I, and the Ft Saint Vrain reactor. In addition to power production, gas-cooled reactors have been suggested as a source of process heat for smelting steel, hydrogen production, and district heating. These large reactors are significantly different in design from the proposed reactor. They generally use a different fuel type and their core geometry was different. TRISO type fuel has been the most common while the British MAGNOX reactors use natural uranium metal encased in a magnesium oxide cladding. TRISO fuel is a pellet sized fuel with layers of silicon carbide and pyrolytic carbon applied to the outside. Most existing gas-cooled reactors use a thermal neutron spectrum and use graphite as a moderator. The proposed reactor will use pins of highly enriched uranium nitride (UN) clad in niobium 1% zirconium (Nb1Zr) in a triangular pitch. These pins will be placed in a prismatic block of Nb1Zr. This limits the comparisons between existing reactors and the proposed reactor somewhat, but comparisons for the remainder of the system should still be useful.

### **2.1.2 How a Gas-cooled Reactor Works**

Gas-cooled reactors are fairly simple systems. The working fluid in a gas-cooled reactor is a single phase gas, which flows across the reactor core [El-Wakil, 1984]. The gas is heated by the fuel pins and then leaves the reactor core. To remove the heat the gas is either run through a heat exchanger transferring the heat to some other working fluid

or, as in this case, run directly through a turbine to generate power. The advantages of gas-cooled reactors are:

- The availability of inert gasses.
- Low neutron cross section.
- The ability to run the reactor at high temperatures.

This last factor allows high efficiency power conversion but requires exotic materials to be practical. As compared to alternative systems, another advantage is the absence of freeze/thaw issues found in liquid metal based systems. The difficulties of managing two phase flow in low or zero gravity conditions are also avoided. However, gas coolants are not as efficient as other coolants in removing heat. While the heat capacity of helium is superior to that of water or many of the common liquid metals on a per-mole basis, the density of helium is so low that appreciable heat removal requires large volumes of gas to be moved across the reactor. This requires careful design for the reactor to avoid large pressure losses. Pumping large volumes of gas also consumes significant amounts of power, reducing the amount available for other purposes.

## **2.2 Brayton Cycle**

A Closed Brayton Cycle will be used for the power conversion system. This cycle has the advantage of being a well understood and robust power conversion cycle.

Extensive testing of similar systems gives confidence in the long-term durability of this system

### **2.2.1 Brayton Cycle History**

Brayton cycle systems have a long history of use and are a well-developed technology. Commercial jet engines use an open Brayton cycle and provided much of the initial data for the first adaptation for space power purposes. Gas-fired turbines for power generation are another application of a Brayton cycle. The development of Brayton cycle systems for space power applications in the US started in the 1960's with NASA's Brayton Rotating Unit program. The goal of the program was to develop a 10.5 kWe Brayton system that could be used with both solar and radioisotope systems [Davis, 1972]. Four different units were tested with a combined 40,000 hours of operation. This program set the stage for a succession of smaller and larger Brayton systems. During the 1980's there was another revival of the program with the intent to deploy a solar-heated Brayton System [NASA, 1993]. Thus, a long standing well tested program gives reason to believe that Brayton Cycle systems are a viable long-life power conversion system for space applications.

### **2.2.2 Brayton Cycle: How It Works**

There are two primary variants of the Brayton cycle: the open cycle and the closed cycle [El-Wakil, 1984]. In an open cycle system, the coolant is drawn in from the outside environment, heated, run through a turbine, and discharged back to the outside atmosphere. In a closed cycle, the gas is in a closed loop and used repeatedly. There are two variants of closed Brayton cycles: direct and indirect. In the direct system, the heat source is directly coupled to the gas flow system while in an indirect system, the coolant passes through an intermediary heat exchanger. A block diagram of a direct closed Brayton cycle is shown below:

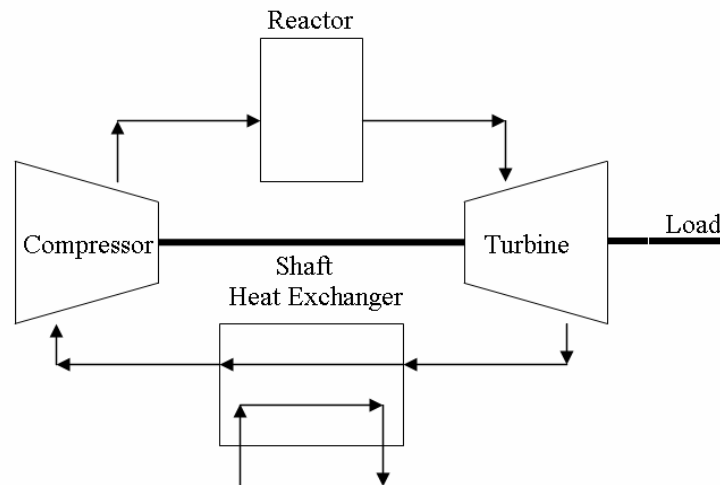


**Figure 2-1 Closed Brayton Cycle [El-Wakil, 1984]**

The working fluid, a single phase gas, is heated in some manner. For gas turbines used as peaking power systems, this means combusting a gas. For reactor-based systems, the gas is run through the reactor core. This gas is then run through a turbine, converting thermal energy into work. The gas is then either vented to the atmosphere (open system) or run through a heat exchanger or radiator to lower its temperature, compressed, and then fed back into the heat source (closed system).

Brayton conversion systems have advantages and disadvantages. They are more efficient than most static power conversion systems (e.g., thermoelectric or thermionic based systems), and they are more durable and simpler than the other dynamic power conversion systems. However, Brayton cycles do require higher temperatures to achieve the same efficiency as other dynamic power conversion systems. The energy density of the working fluid is low compared to the other dynamic power conversion systems.

Single point failure can be a problem with Brayton systems. A leak in the reactor can easily lead to all the coolant being lost.

### **2.3 Fast Spectrum Reactor**

The decision to focus on a fast spectrum reactor was largely a result of the desire for a high temperature gas outlet. The higher temperature of the gas increases the efficiency of the Brayton cycle. Thermal systems tend to be larger than fast systems. Thermal spectrum systems require moderators, and efficient moderators tend to be hydrogen-based and most are not compatible with high temperatures. Two possible high temperature moderators are yttrium hydride and graphite. Yttrium hydride is a hydrogen-based, high temperature moderator that is currently being examined. It has some serious unknowns associated with it including the long-term effects of being at the desired elevated temperatures in a high-radiation environment and the temperature feedback coefficient. Graphite is much less efficient at moderating neutrons and would likely increase the size of the reactor significantly. This makes fast spectrum reactors favorable if high temperature outlet gases are desired.

Fast Spectrum reactors use high energy neutrons ( $>100$  keV) to initiate fission. There are a variety of complications associated with this. At these higher energies, fission cross sections drop from the multi-hundred barn range into the low single digit range, reducing the reaction rate significantly. Thus for the same power output, a fast reactor needs to have a much higher neutron flux than a thermal reactor. This tends to accelerate radiation induced damage to other components of the reactor. On the other hand, the relative magnitudes of the cross sections of materials mean that most materials are relatively transparent to fast neutrons. Boron, rhenium, and a variety of other

materials that are poisons in the thermal spectrum have a far smaller impact on fast neutrons. The method for controlling the reactor is external reflectors. The position of the reflectors is used to adjust the leakage of the system. Other than a slight diversion into what a thermal spectrum reactor would look like, the vast majority of this project will be done for fast cores.

## **2.4 Fuel**

The fuel type selected for the core is highly enriched UN because UN has been tested to a greater degree than uranium carbide, which is theorized to have similar characteristics. The thermal properties of UN are favorable as compared to UO<sub>2</sub>; the only fuel type that has been tested to a greater degree. UN is a better choice than the TRISO type fuel typically used in gas-cooled reactors because of the low relative uranium density (7-8% of UN) of TRISO. One of the primary advantages of TRISO type fuels is the high achievable burnup. As high burnup of the fuel is not one of the design goals, TRISO's primary advantage is negated. TRISO's reduced uranium density would necessitate an unacceptable increase in core size. Testing has shown that UN is a viable material at the expected burnup for this core.

The fuel in the reactor will be 93% enriched UN. The decision to use Highly Enriched Uranium (HEU) for fuel is partially a result of the lifespan related considerations. Ten years at 200- 400 kW thermal power would consume 0.8-1.6 kg of <sup>235</sup>Uranium. With the proposed highly enriched system this is only 0.86% of the fuel, which is a small burnup. The reactivity swing associated with this burnup was determined to be 0.006 (~1\$), and sufficient extra fuel needs to be in the core to compensate for this reactivity swing. HEU does increase the security related costs for the

reactor. One minor alternative designed to mitigate this cost for a nuclear heated ground test facility is examined in the alternative cores section.

## **2.5 Pin Type Geometry**

The fuel pins used in the core are a new type for GCR's. The vast majority of GCR reactors use a TRISO type fuel embedded in a graphite matrix and are thermal neutron spectrum reactors. TRISO fuels are small UC spheres coated with layers of silicon carbide and pyrolytic carbon. While this results in fuels that can be used to extremely high burnup, the uranium density of the fuel is low. A coolant hole is then drilled through the blocks of fuel and these blocks are put in a prismatic array.

The proposed reactor uses an array of UN pellet filled pins in a triangular pitch. These pins are clad in a layer of rhenium and Nb1Zr. The use of rhenium limits the problem of nitrogen attack on Nb1Zr. It also has positive accident safety characteristics. These pins are similar to those developed for the SP-100 program though they are used in a different reactor setup.

## **2.6 Space Environment**

This reactor is intended for use on Mars. Unlike many other extraterrestrial environments, Mars has an atmosphere. Specifically the atmosphere is roughly 4-7 millibar of pressure and composed of 95% carbon dioxide, 2.7% nitrogen, 1.5% argon, 0.15% oxygen, and 0.15% water (Keifer, 1992). This presents a host of complications for materials choices in the reactor. The pressure vessel of the reactor will be exposed to this environment while at an elevated temperature. While this temperature is lower than what one would expect for a liquid metal or rankine cycle reactor, it is high enough to

accelerate reactions. The interaction between the environment and the outer surfaces of the reactor is a problem that will not be examined in this work. Oxidation and other reactions will cause problems for reactors and must be considered. For example, at the likely temperature for the pressure vessel (876 K), Nb1Zr absorbs oxygen from the atmosphere readily and becomes brittle [DiStefano, 1990]. The material used on the exterior of the reactor needs to be resilient enough to last the expected 10 years in the given environment. This tends to eliminate many of the high temperature refractory alloys which have oxidation problems.

### **3 Materials Used in the Design**

A variety of relevant properties at the estimated temperatures for the given material will also be examined. There are three general classes of materials in the reactor: Metals, Ceramics, and Gasses.

#### **Metals**

For all the metals several properties will be examined. The mechanical properties are Yield Strength (YS), Ultimate Tensile Strength (UTS), and Creep Strength Vs Temperature. The thermal properties that will be examined are thermal conductivity and linear expansion.

#### **Ceramics**

For the Ceramic Materials, the mechanical property that will be examined is the Modulus of Elasticity. The thermal properties that will be examined are thermal conductivity and linear expansion.

#### **Gasses**

The helium/xenon coolant will be compared relative to some other common gasses. The properties that will be examined are viscosity, thermal conductivity, specific heat and density.

#### **3.1 Uranium Nitride**

UN is a ceramic mixture of uranium and nitrogen. It has a melting point in the range of 3100 K, well above the likely peak fuel temperatures (1300 K) [Tagawa, 1974]. The maximum theoretical density is 14.32 g/cc [Johnson, 1976]. The core will use a 1-to-1 atomic ratio mixture. A phase diagram for UN can be found in Figure 3-1.

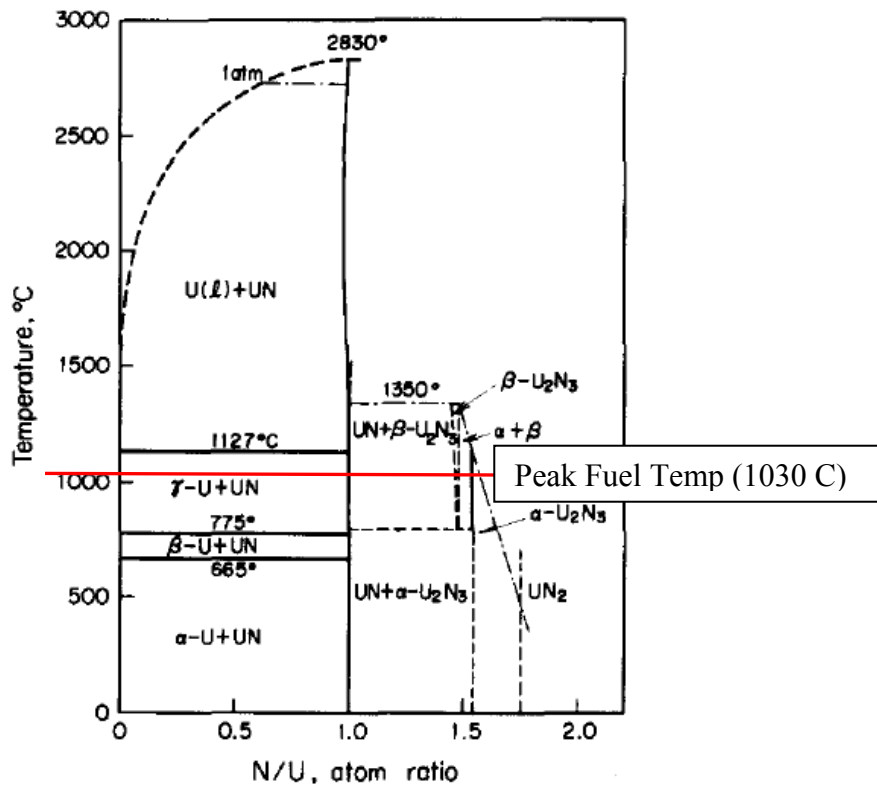
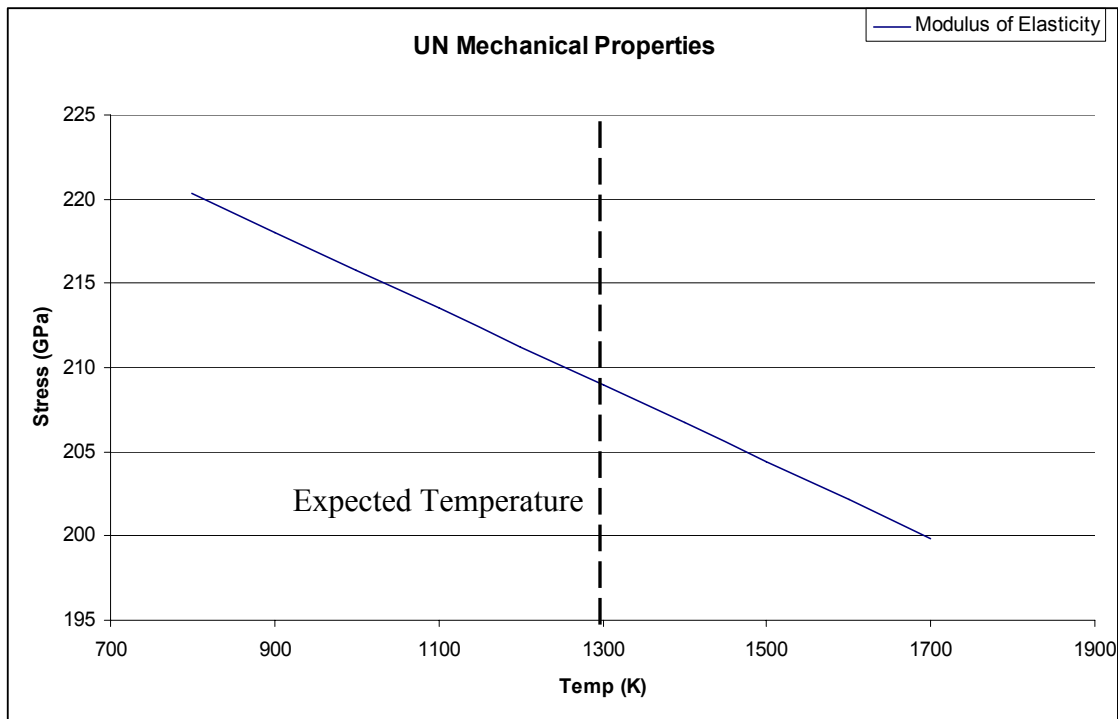


Figure 3-1 UN Phase Diagram [Tagawa, 1974]

## Mechanical Properties



**Figure 3-2 UN Mechanical Properties**

## Thermal Properties

There are a variety of advantages to using uranium nitride (UN) over the other fuel types, and a handful of drawbacks that need to be considered. Uranium nitride has a much higher thermal conductivity than uranium dioxide, resulting in a flatter temperature profile across the fuel pin. The same is likely true for uranium carbide, but less testing has been done on uranium carbide than for UN. Figure 3-3 shows the desired thermal properties of UN [Touloukian, 1979]. At the operational temperature, 1300 K, the thermal conductivity is 28.5 W/m-K and the linear expansion is roughly 1%. It is important for the different components to expand at similar rates to minimize the extra stresses.

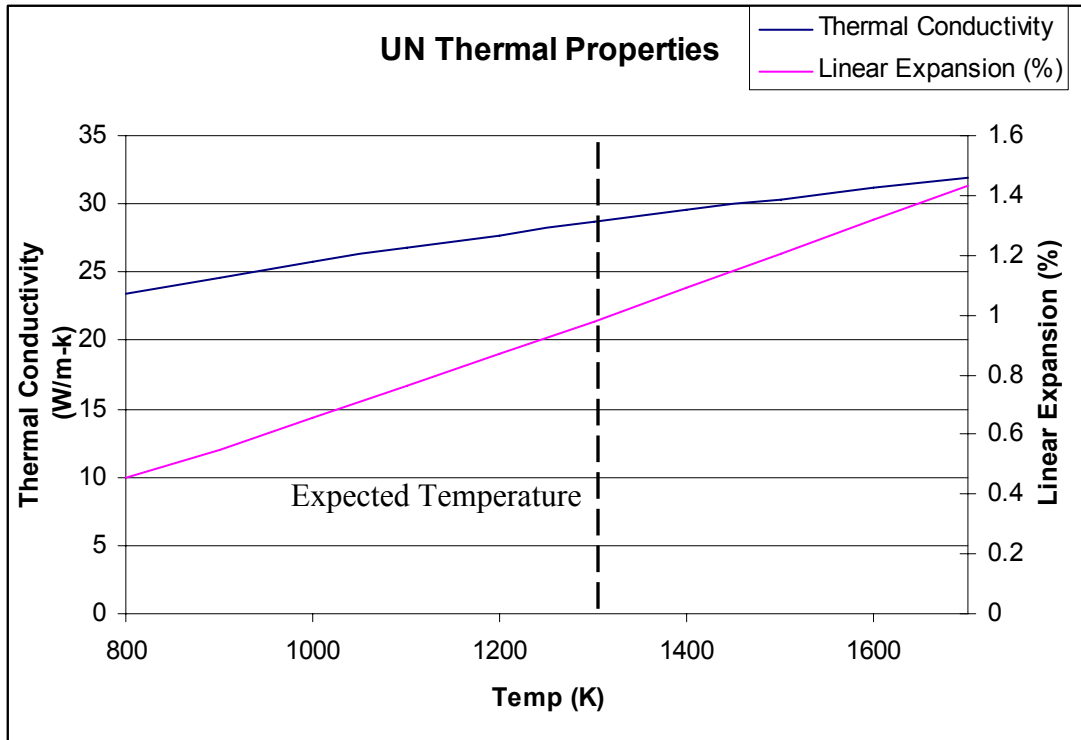


**Figure 3-3 UN Thermal Properties**

### Additional Considerations

There are contradictory statements on fission fragment retention from different sources. There is a general statement that UN retains fission fragments better than  $\text{UO}_2$ . In personal discussions others have indicated that the oxygen released due to fission for  $\text{UO}_2$  systems has a tendency to bind with several types of fission fragments into an oxide that does not migrate [Lenard, Roger and Lipinski, Ronald, personal communication, August 2005]. While the latter does not necessarily invalidate the general sweep of the former statement, it does highlight the difficulties in making sweeping generalizations.

In this design, the UN fuel will be located in the drum of the core, clad in a layer of rhenium and niobium 1% zirconium. This rhenium layer is required because of incompatibilities between nitrogen and niobium 1% zirconium. The nitrogen out-gassing

and the fission gasses that are not bound by the nitrogen aggressively attack Nb1Zr cladding, leading to breaches into the clad. There is evidence that this problem is widespread across a variety of materials. The effects of irradiation on UN are still not completely understood.

### **3.2 Helium/Xenon**

The coolant chosen for the reactor will be a mixture of helium and xenon. There are two primary reasons for choosing a mixture: the limitations related to machining components and the favorable thermal characteristics of He/Xe mixtures. The vast majority of the parameters that go into determining the turbine and compressor wheel size are fixed by other limitations. If a low molecular weight gas is used, the size of the turbine wheel will end up being small. The tolerances between the wheel blades and the cowling are the same regardless of the wheels size so for a smaller wheel the magnitude of the losses goes up drastically. [Steven Wright, personal communication, March 20, 2006] One method of avoiding these losses is to use a heavier gas. Heavier gasses tend to have lower heat capacities. Mixtures of helium and xenon have favorable thermal characteristics when compared to argon and neon. A mixture of helium and xenon can have the same average molecular weight as argon or neon but have better heat transfer characteristics than either one. A mixture of helium and xenon with an average molecular weight of around 40 g/mol seems to be a very common choice [Angelo, 1985]. Table 3-1 shows properties of helium, xenon, the proposed mixture, and other gases for comparison. The properties for all the gases except for xenon were taken at 1000 K and 2 MPa. Xenon was taken at 800K due to limitations of the reference.

**Table 3-1 Gas Properties [1] [2]**

	Helium [1]	Xenon [1]	He/Xe [2] (70/30)	N2 [1]	CO2 [1]
Density (kg/m <sup>3</sup> )	0.96	39.46	7.5	6.69	10.5
Specific Heat (Cp) (J/mol-k)	20.78	21.151	20.52	32.75	54.5
Gamma	1.67	1.69	1.676	1.34	1.18
Viscosity (μPa-s)	46.17	54.908	65.2	41.68	41.31
Thermal conductivity (W/m-k)	0.3617	0.01319	0.15446	0.0661	0.0708

[1] From NIST Chemistry Webbook, <http://webbook.nist.gov/chemistry/>

[2] From Lipinski, 20002

This table shows that helium has the highest thermal conductivity with the helium/xenon mixture coming in second.

### **3.3 Niobium 1% Zirconium**

Niobium 1% zirconium is an alloy of 99% niobium and 1% zirconium with a melting point of Nb1Zr is 2673 K and a density of 8.64 g/cc at room temperature [Summary, 1965]. Nb1Zr is a robust alloy that retains its strength up to high temperatures. The nominal temperature limit for the alloy is 1350 K. The expected peak temperature for Nb1Zr as a cladding is 1300 K, below its nominal limit.

## Mechanical Properties

Figure 3-4 shows the operational domain of Nb1Zr with vertical line showing the expected operating temperature 1300 K.

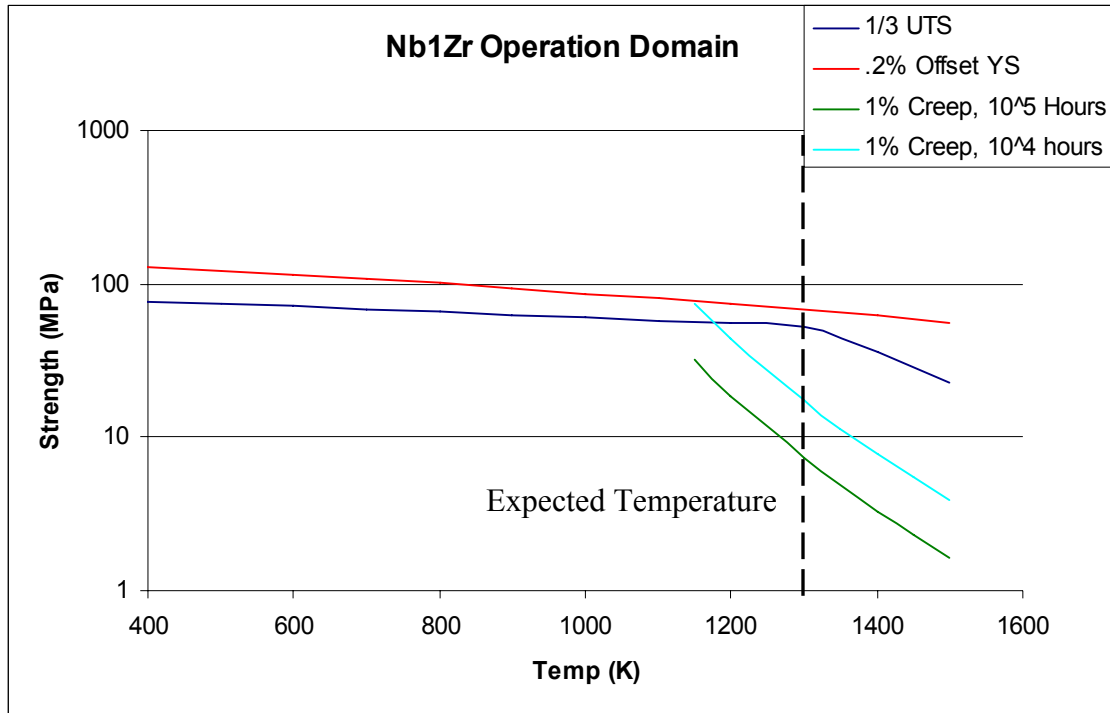


**Figure 3-4 Nb1Zr Operational Domain**

This chart represents minimum values expected for Nb1Zr [Summary, 1965] [Watson, 1965]. Several other sources listed higher values for both the yield strength and tensile strength; some by as much as 30% [Niobium, 2006]. This plot shows that at the expected temperatures, the maximum yield strength is roughly 68 MPa and the 1/3 tensile strength limit is 52 MPa. In any event, at the desired temperatures, neither of these properties is the limiting factor; creep strength is. The 1% creep strengths of Nb1Zr in a liquid lithium environment are also shown in Figure 3-4. While the Nb1Zr will be in a He/Xe environment, it was the best data available. The 1% creep limit at 10<sup>5</sup> hours (roughly 11 years of continuous operation) shows the stress limit on the niobium 1% zirconium

[Horak, 1985] is about 7.38 MPa. Of the possible limiting stresses for the metal this is the lowest at 1300 K and thus becomes the limiting property for Niobium 1% Zirconium.

### Thermal Properties

The thermal conductivity of Nb1Zr at 1300 K is 69 W/m-K [Touloukian, 1970]. The linear expansion of Nb1Zr at 1300 K is 1% [Touloukian, 1975]. Figure 3-5 shows linear expansion and thermal conductivity as a function of temperature.

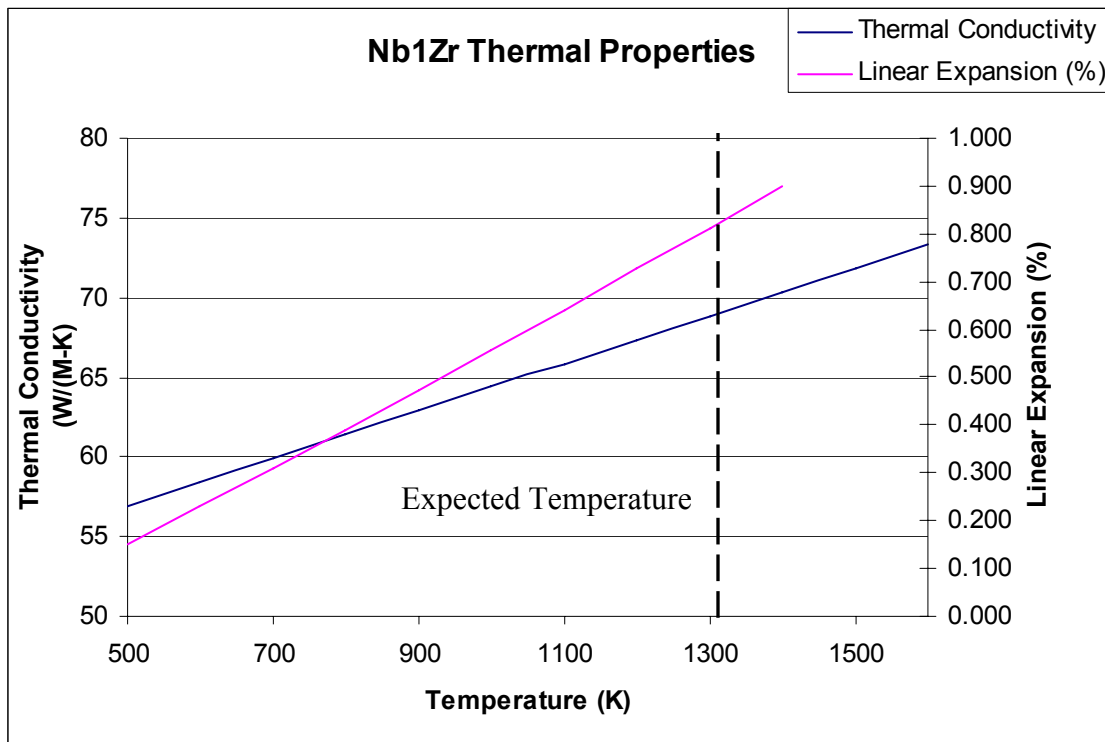


Figure 3-5 Nb1Zr Thermal Properties

### Additional Considerations

There are some limitations to Nb1Zr based alloys. At high temperatures Niobium oxidizes rapidly in atmospheres containing oxygen, resulting in significant embrittlement [DiStefano, 1990]. This restricts the use of Nb1Zr when in contact with most atmospheres. These limitations preclude the use of Nb1Zr on the outside surfaces of the

reactor. The strength of Nb1Zr is also limited. There has been little indication that such a breakthrough has been made to date.

### **Alternatives worth Pursuing**

There is a slight variant called PWC-11 that introduces 0.1% carbon into the Nb1Zr alloy. This increases the creep strength properties by 30-40% while not changing the thermal properties. It would probably merit further investigation as a material choice.

### **3.4 Hastelloy X**

Hastelloy X (HastX) is a nickel-based superalloy used in a variety of applications [Brown, 1992]. Its composition is 49% nickel, 22% chromium, 18% iron, 9% molybdenum, 1.5% cobalt and 0.5% tungsten. The melting point of HastX is about 1530 K, and it has a density of 8.22 g/cc. This material has been suggested as a possible reactor material for a variety of reasons. HastX is a material with decent high temperature characteristics. Hastelloy is also noted for excellent corrosion, oxidation and carburization resistance at the desired temperatures. Finally, Hastelloy-X is a commonly used metal whose properties are well understood. The expected peak temperature of Hastelloy-X is roughly 875 K when used for the pressure vessel of the reactor.

## Mechanical Properties

Figure 3-6 shows the Yield Strength, 1/3 UTS, and 1% creep at 10000 hours (approximately 1 year).

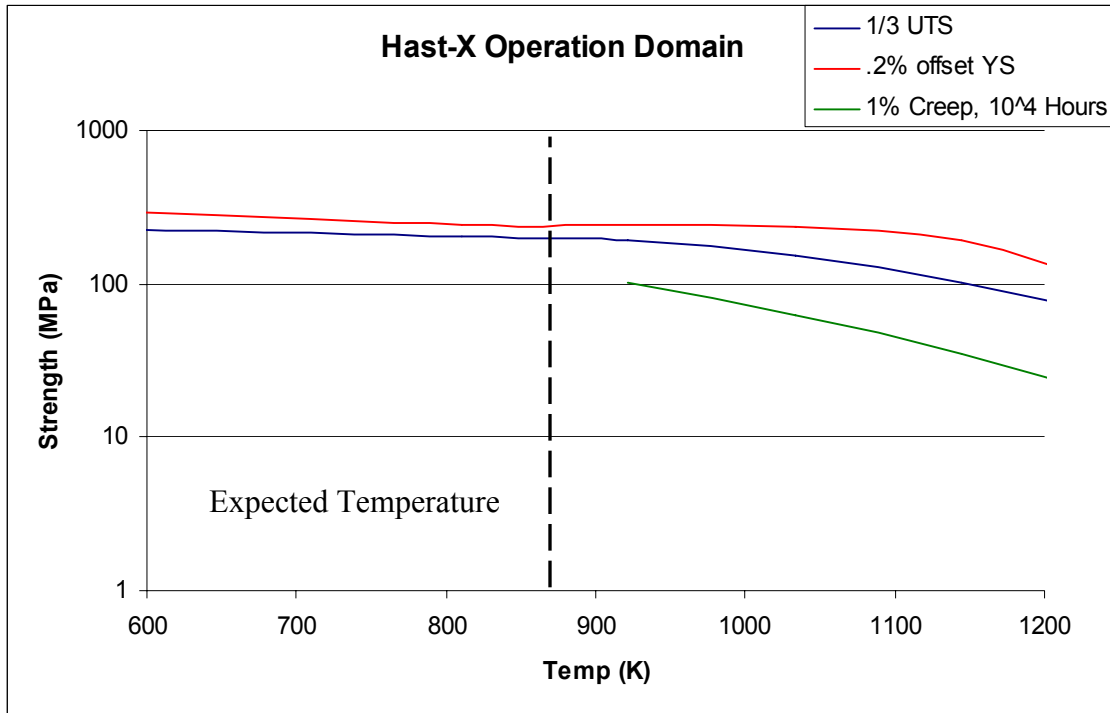


**Figure 3-6 Hastelloy X Operational Domain**

There are some notable limitations to this data. The 1% creep data for 10<sup>5</sup> hours was not available. The 10<sup>4</sup> hours creep data did not extend to the desired temperatures. The 1/3 UTS is roughly 195 MPa and the 0.2% offset yield strength was 245 MPa at 860 K. In all likelihood, all three limits are close to the same value at the expected operation temperature. The creep strength is constraint most likely to be exceeded

## Thermal Properties

The thermal conductivity of HastX is 20.8 W/m-K at 860K and the linear expansion is 0.8%, as shown in Figure 3-7.

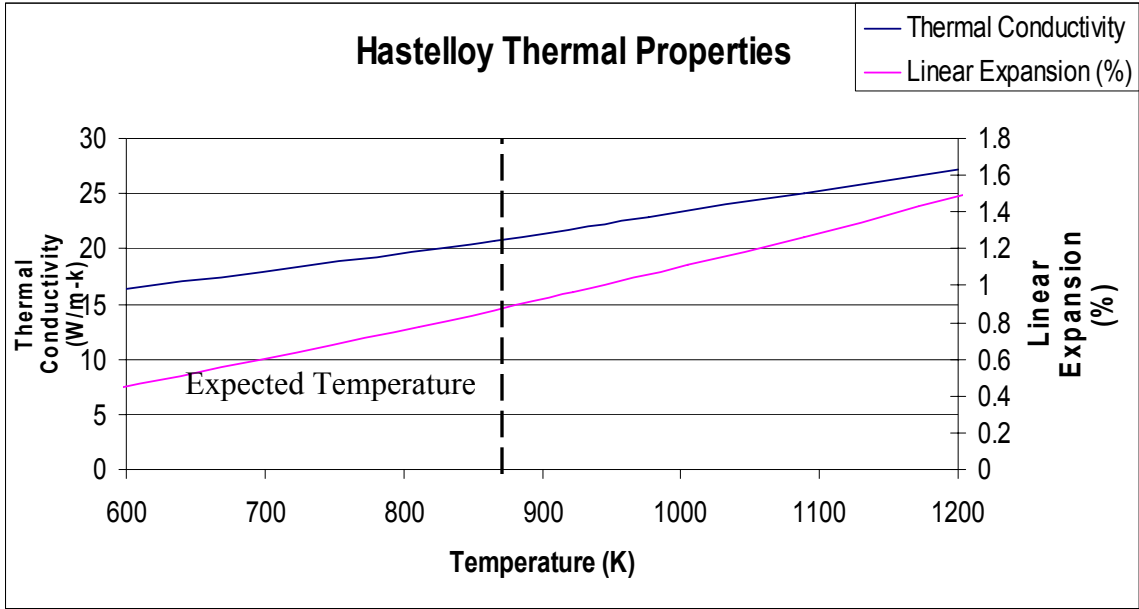


**Figure 3-7 HastelloyX Thermal Properties**

### 3.5 Beryllium Oxide

BeO is a ceramic with a 1-to-1 atom ratio of beryllium to oxygen. It is primarily used in the nuclear field as a neutron reflector. The oxygen component results in BeO being an extremely good scattering material as it has a very high scattering to absorption cross section ratio. In addition to being a reflector, there is an n-2n reaction in beryllium that increases neutron numbers, increasing this material's attractiveness. BeO will be located in two different regions of the core with drastically different temperatures. In the individual fuel pins, axial reflectors of 5 cm BeO at the pin ends will be at around 1300 K. The radial reflectors will be at some temperature between 860 K and the environmental temperature.

## Mechanical Properties

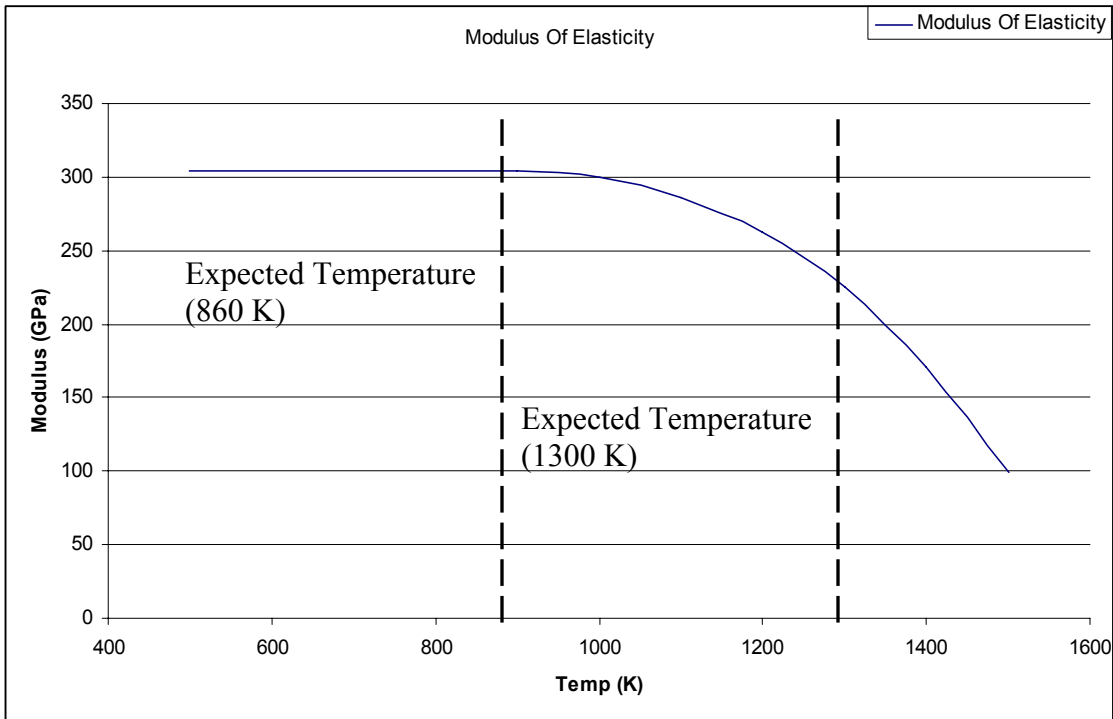


**Figure 3-8 BeO Mechanical Properties**

## Thermal Properties

BeO has a thermal conductivity of 0.635 W/cm-K at 860 K and 0.28 W/cm-K at 1300 K.

The linear expansion is 0.45% at 860 K and 0.912% at 1300 K

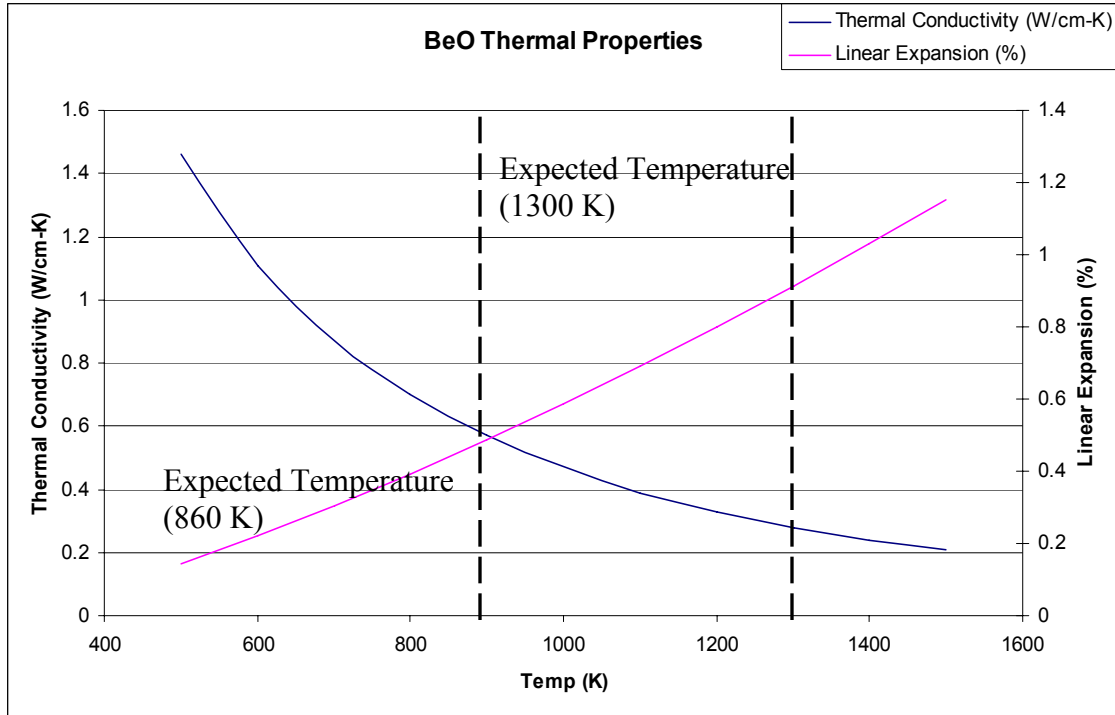


**Figure 3-9 BeO Thermal Properties**

### 3.6 Rhenium

Rhenium is a super dense refractory metal that will be used in a non-structural capacity in the reactor. Its melting point is 3459 K, and its density is 21 g/cc. There are a variety of characteristics of rhenium that make its use a challenge. There seems to be a great deal of variability in the mechanical properties of rhenium, depending greatly on the methods used to prepare the sample [Biaglow, 1995]. All of these things complicate any attempt to use it in the reactor, but the amount of rhenium in the core is limited and not used in a structural capacity. Rhenium is used as a liner 0.062 cm thick between the cladding and the fuel. Thermally speaking, there is an almost negligible drop of temperature across the liner. Rhenium is not used as a structural material so its

mechanical properties are not that important. The thickness of the rhenium layer is so thin that its thermal properties have a minimal impact on the core.

### **Attractive Features**

One of its attractive features of rhenium is that it is a spectral shift absorber (SSA), which means that it has a low relative absorption cross section for fast neutrons; while in the thermal spectrum its absorption cross section increases dramatically. This has safety applications for the reactor design in accident scenarios. Rhenium has an absorption cross section of  $\sigma_a$  in the fast spectrum, however the magnitude of the difference between the absorption cross section and the fast fission cross section of  $^{235}\text{U}$  is low compared to the difference at a thermal spectrum. It also provides a barrier that protects Niobium 1% Zirconium from nitrogen attack and damage caused by other fission products that outgas from the fuel. Most of the other SSA materials have a relatively low melting point, making them less attractive.

## 4 Design Description

### 4.1 Design of Reactor

The original parameters of the reactor design were derived from an internal study done by Ron Lipinski, Dan Dorsey et al. for an earlier project. The general goal of that project was to explore the region in which a gas-cooled pin type reactor was practical. They did a number of runs where the radius of the fuel, thickness of the rhenium liner, thickness of the cladding, and number of fuel pins were varied. However, the runs were limited calculations at room temperature. The dry sand accident case was not examined, and there was no attempt at optimizing the designs. Parametric scans showed the multiplication factor for these cases, and the results provided a starting point for the reactor dimensions. The effect of the reflector position on the reactor multiplication factor was not examined either. Unfortunately this work was not published but the results were available to the author.

What this thesis will do is:

- Examine the effect of the reflector on the reactor
- Determine the temperature effects on the core
- Optimize the primary core for the three accident scenarios
- Examine alternate cores for
  - Reduced testing costs (Cat-III cores)
  - Enhanced Launch Safety (Internal Control Rod)
- analyze Quality Control runs to better understand the inner workings of the reactor

- Look at the effects of the radiator on the Brayton cycle efficiency and system mass.

One of the initial considerations was the desire to keep the UN fuel pellets similar to those used on the SP-100 project as it was known that fuel could be manufactured at those dimensions. This fixed the number of fuel pins and other parameters. The reactor is controlled with external reflectors that move axially to open up a gap between the upper and lower reflectors, increasing the leakage of neutrons from the center of the reactor. The fuel is cooled by a 70/30 molar fraction Helium/Xenon gas mix. Table 4-1 shows a variety of parameters for the reactor:

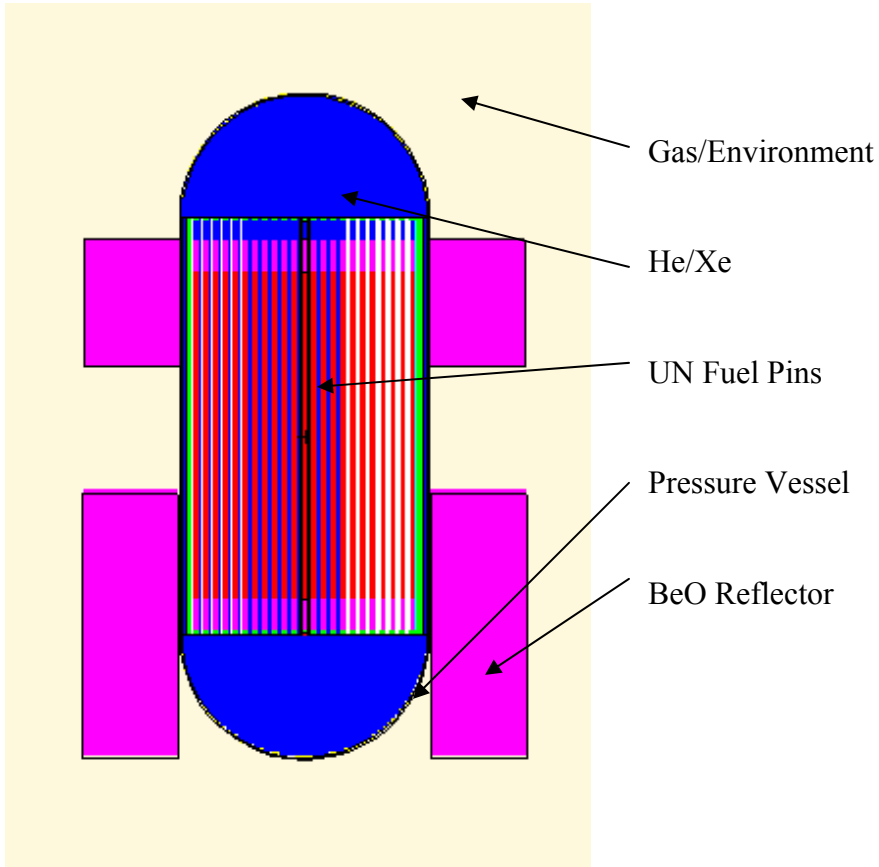
**Table 4-1: Primary Core Parameters**

Core	Primary Design
Gas Properties	
Coolant	He/Xe
He fraction	70/30
Reactor Core, Vessel, Reflectors	
Type	Pin-matrix
Reactor Material Properties	
Fuel material	UN
Clad material	Nb1%Zr
Clad liner material	Re
Wire wrap material	Re
Moderator material	N/A
Matrix (core block) material	Nb1%Zr
Pressure vessel material	HastX
Radial reflector material	BeO
Axial reflector material	BeO
Lower grid material	Nb1%Zr
Upper grid material	Nb1%Zr
Coolant material	He/Xe
Fissile material	U-235
Fuel enrichment	0.9315
Reactor Radial Dimensions	
Radius of the fuel (UN only) (m)	4.54E-03

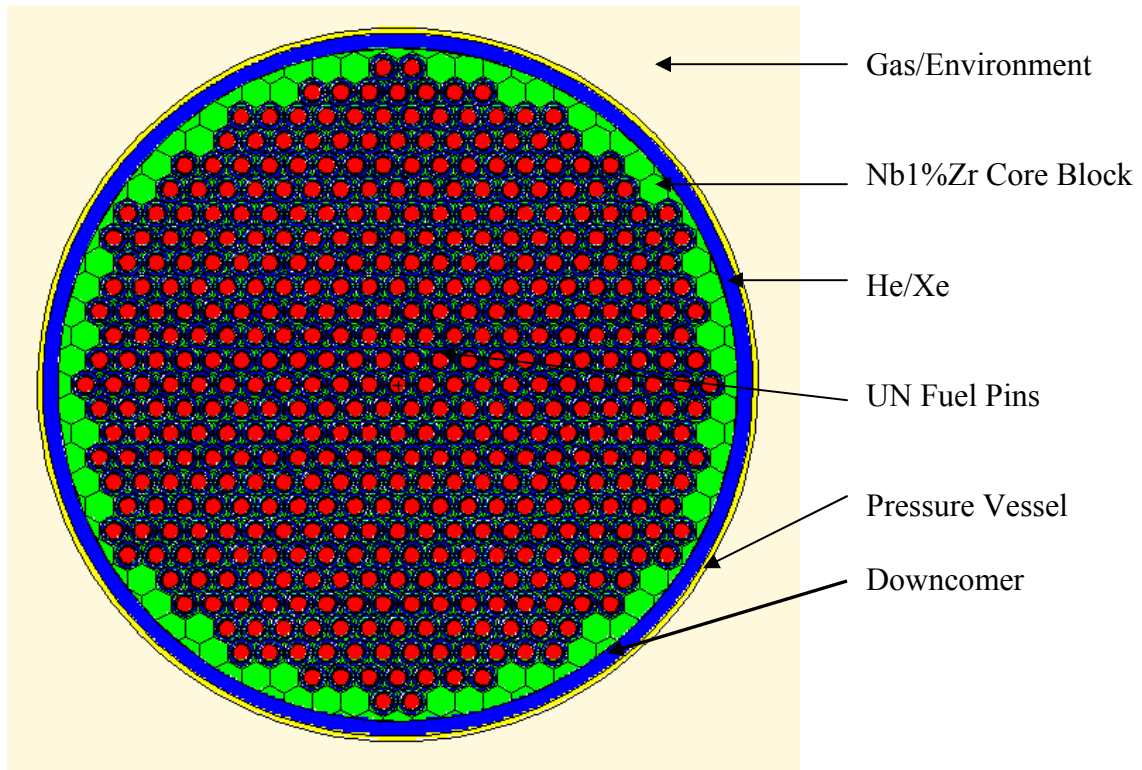
Thickness of the fuel gap (m)	6E-05
Thickness of the liner (m)	6.2E-04
Thickness of liner-clad gap (m)	4E-05
Thickness of the clad (m)	4.4E-04
Thickness of coolant channel (m)	1.65E-03
Width to thickness ratio of rectangular wire	1
Pitch of the wire wrap (m)	0.2
Number of wires wraps per pin	2
Thickness of matrix between pins (m)	7.8E-4
Number of fuel pins	451
Thickness added to circle to get matrix radius (m)	0.016
Thickness of matrix insulation (He/Xe) (m)	0.0002
Thickness of the matrix & dome baffle (m)	1E-06
Thickness of the downcomer channel (m)	0.008
Thickness of the pressure vessel (m)	0.003
Thickness of the reflector gap (m)	0.001
Thickness of the radial reflector w/o clad (m)	0.15
Reactor Axial Dimensions	
Length of the active fuel in the reactor (m)	0.52
Length of the axial fuel plenum (m)	0.03
Length of upper axial reflector (m)	0.05
Length of lower axial reflector (m)	0.05
Length of each end cap (m)	0.005
Length of the lower grid plate & pin flow orifices (m)	N/A
Length of the outlet (upper) plenum (m)	0.005
Length of the inlet (lower) plenum (m)	0.005
Other Properties	
Axial peak-to-avg ratio in core	1.2

Radial peak-to-avg pin power	1.2
SiO2 fraction in wet sand	0.64
K-Effective of Core	1.037 ±0.001

The following are graphics showing the reactor as analyzed. Figure 4-1 shows an axial cross section of the reactor with the reflectors partially open.



**Figure 4-1 XZ Plane Section of Reactor**



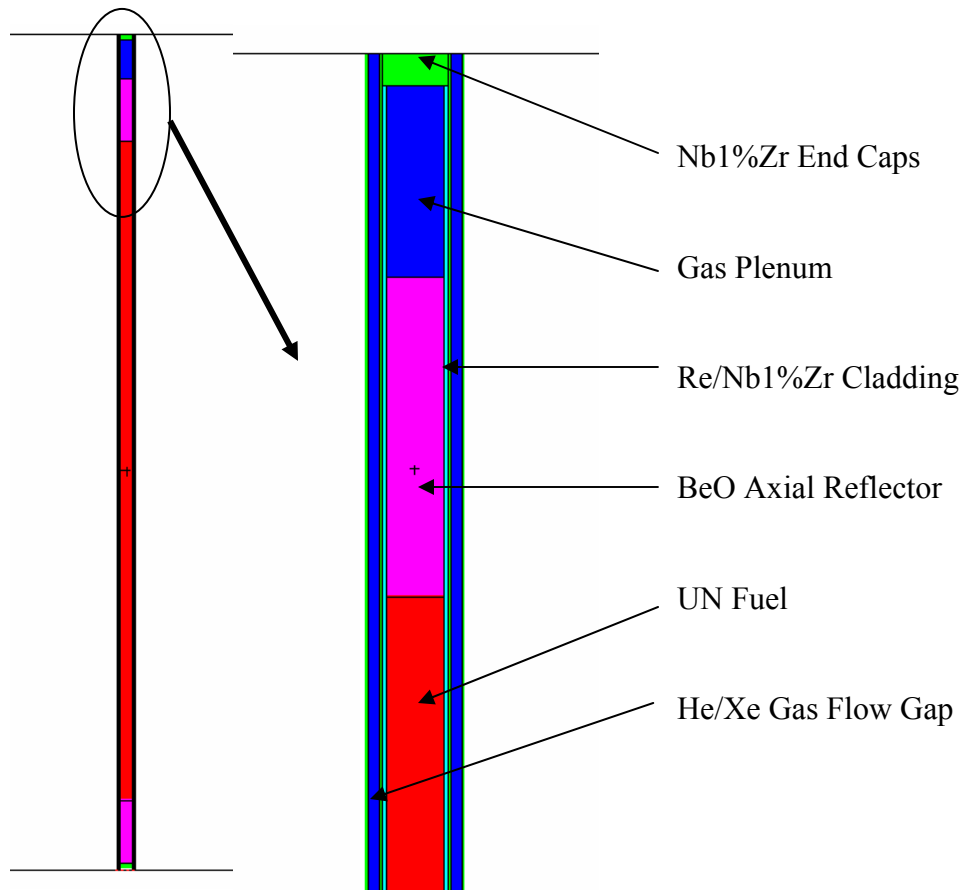
**Figure 4-2 XY Plane Section of Reactor**

Figure 4-2 shows an XY plane of the reactor core without the radial reflectors. Moving in radially we see:

- The pressure vessel of the reactor
- The downcomer that the cold inlet gas flows through
- The core block with the fuel pins suspended in it

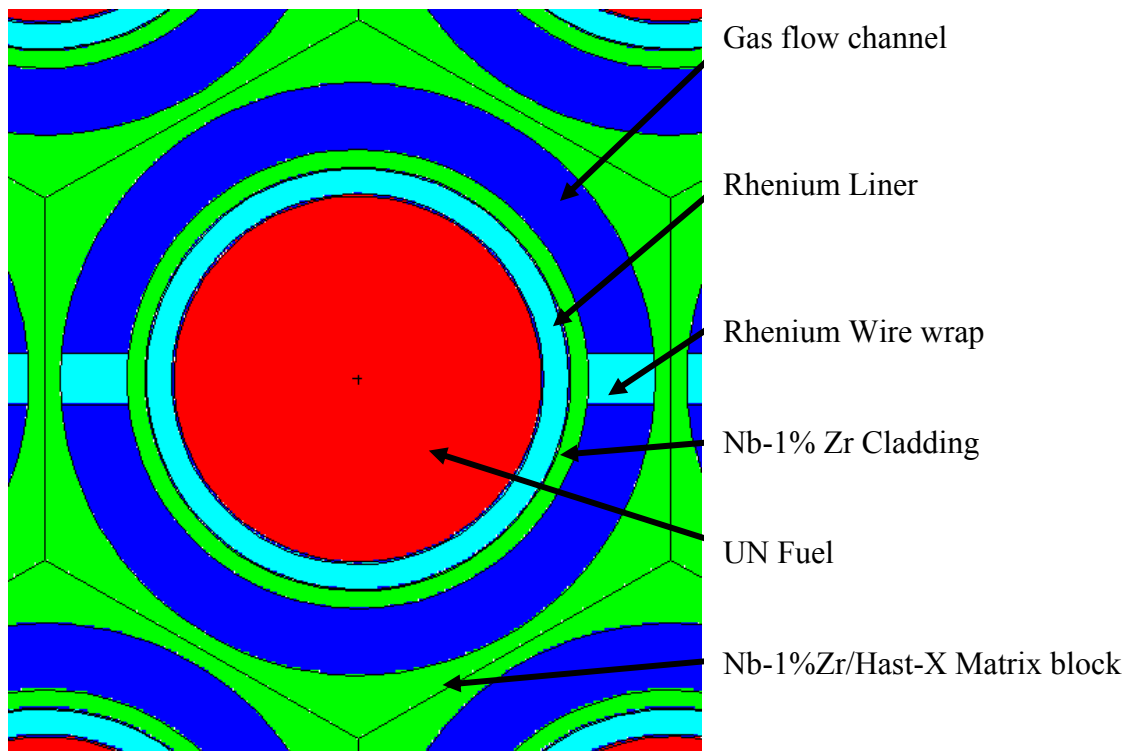
Flowing coolant through the downcomer keeps the surface of the reactor at a lower temperature. The diameter of the barrel of the core without the reflectors is 19.5 cm.

Figure 4-3 shows an axial slice of a single fuel pin with a close-up of the end cap section.



**Figure 4-3 XZ Plane Section of Individual Fuel Pin**

The fuel consists of a series of UN pellets that are total of 52 cm in length and 0.91 cm in diameter. These are capped by 5 cm of BeO to act as an axial reflector. There is a gas plenum on the top of the pin to allow for fission product gas build up. A layer of rhenium acts as a liner for the fuel pin to prevent interaction between the Nb1Zr cladding and the UN pellets and also acts as a thermal neutron absorber in accident cases as discussed later. The Nb1Zr end caps appear large in this Figure but their purpose is to simulate other components like the connectors that attach the fuel pin to a grid plate.



**Figure 4-4 XY Plane Section of Fuel Pin**

The XY plane section of a pin shows a close-up of the radial layout of a single pin. The innermost volume of the fuel pin is UN. Then there is a small gas gap followed by a layer of Rhenium. Next is the Nb1Zr cladding and then the gas flow channel. Finally there is the matrix that the fuel pins are suspended in. A rhenium wire wrap is used to keep the fuel pins centered in the flow channels.

## 4.2 Gas Flow in Reactor

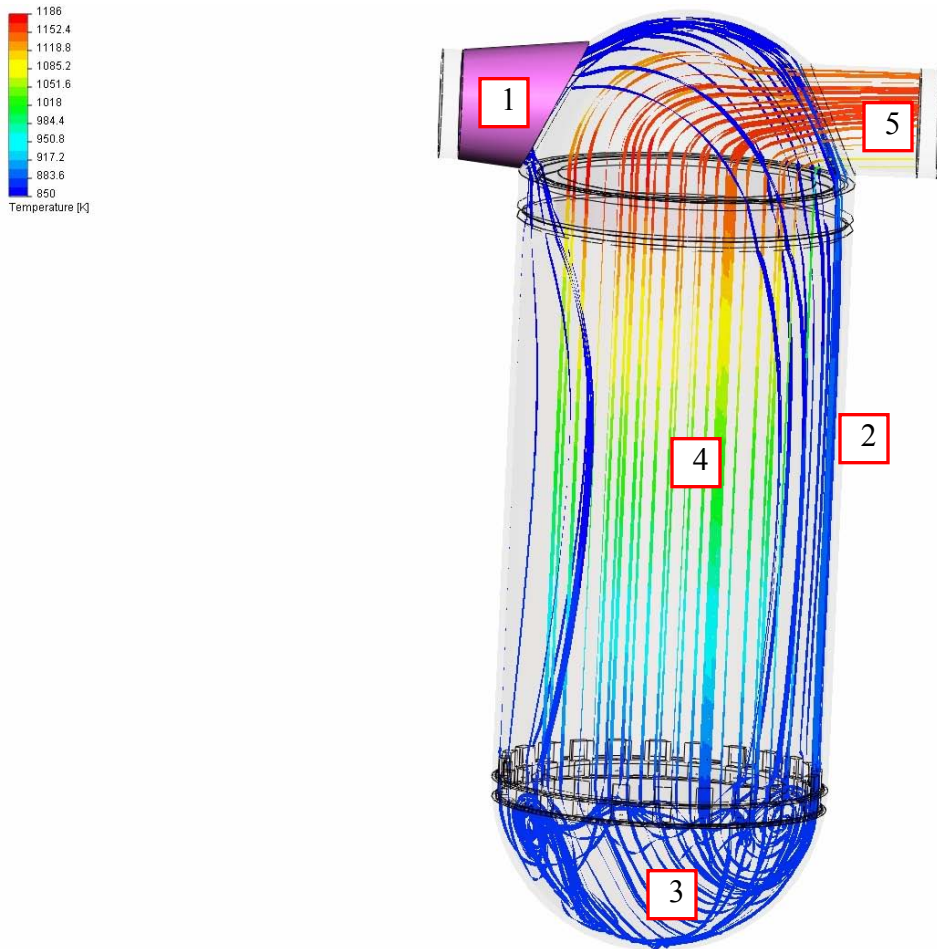


**Figure 4-5 Flow Pattern for Reactor**

One of the more interesting characteristics of the reactor is how the flow pattern is used to cool the pressure boundaries of the reactor. Figure 4-5 of a similar reactor and used only for illustration purposes [Brown, N., 2006]. The exterior of the reactor is made out of HastX, which has a much lower tolerance for high temperatures than the Nb1Zr that makes up the bulk of the reactor, thus the need for cooling. The top hemisphere of the reactor is actually two separate shells. Cold gas flows in through the outer shell (1). It

then passes through an annulus on the outside edge of the fuel pin matrix(2). This keeps cool inlet gas in contact with the outer pressure vessel reducing its temperature to 850 K from the 960K of the outer surface of the fuel pin block. In the bottom hemisphere, it then loops around (3) and is forced up through the coolant channels around the fuel pins (4). Finally the gas exits the top of the reactor on its way to the turbine (5).

### **4.3 Pressure Vessel Composition: Hastelloy-X**

As a result of the desire for a pressure vessel material compatible with the Martian environment at the desired temperatures Hastx was chosen for the pressure vessel. HastX is known for being extremely insensitive to corrosion and carburization [Brown, W., 1992]. Theoretically, the relatively small neutronic penalty associated with Hastelloy means that any comparably transparent material (from a neutronic standpoint) could be substituted, which may be necessary if HastX and Nb1Zr are incompatible.

### **4.4 Core Block Composition**

Initially a decision was made to make the core block (the matrix of material that the fuel pins sit in) out of either HastX or Nb1Zr. There is little neutronic difference between the two materials. The deciding factor between the two is the peak temperature in the core. If a lower temperature (and efficiency) is acceptable, then HastX is probably the better choice. Niobium 1% Zirconium is the higher-temperature alternative. To achieve higher efficiency the core block of the reactor will be made out of Nb1Zr. At 100 kWe the temperature in the block is high enough that the long term creep strength of HastX is a concern.

#### 4.5 Reactor Control Methods

The reactor will be controlled with external reflectors that slide axially up and down along the reactor creating a gap adjacent to the active fuel length of the reactor as shown in Figure 4-6.

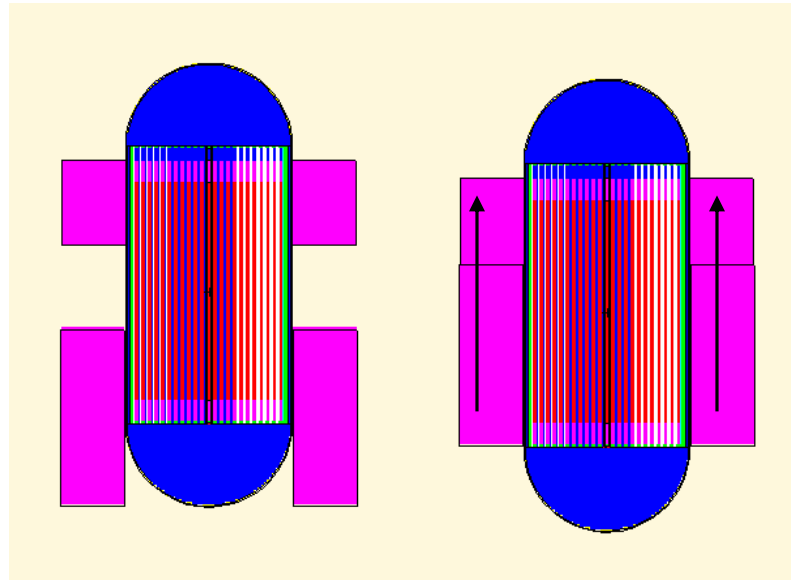


**Figure 4-6 Reflector Movement**

Movement of the reflector elements increases or decreases the leakage of the reactor, allowing for control of the neutron population. The reflector is made with two separate components: the moveable reflector and the fixed reflector. The upper one-third of the reflector is fixed in place forming an annulus around the upper part of the reactor. The lower moveable section provides variable leakage for control of the reactor core. The gap where the reflectors open up is in a region of relatively high flux so small changes in reflector position have a larger impact on the leakage. The moveable reflector consists of eight separate segments to minimize the risk of mission failure should a moveable reflector fails. The eight segments of the reflector are shown in Figure 4-7.

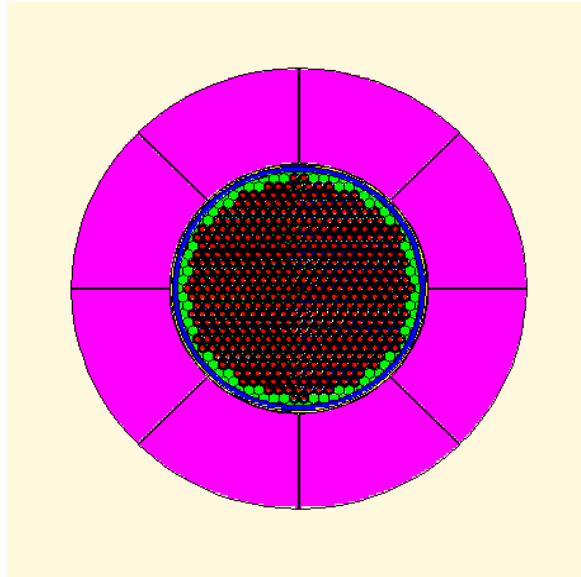


**Figure 4-7 XY Plane Section with Radial Reflectors**

Separating the reflector into segments is a good idea because during launch the reflectors will be ‘open’ and having one stick would reduce the useable life of the reactor by limiting the available reactivity swing. If a reflector were to stick in the ‘closed’ position the problems are lessened; there is still a significant amount of reactivity swing available from moving the remaining blocks. There is a chance that the reactor will initially have a ‘safety block’ along the centerline of the core to ensure sub-criticality while the system is being launched, but control of the reactor after launch will be done solely with external radial reflectors.

## 5 Neutronic Investigation into Core Design Results

To examine its viability, a variety of parametric scans were performed using MCNP-5 [LANL, 2003] on a model of the proposed core. The core was designed with sufficient reactivity to ensure 10 years of full-power operation even when including such negative feedback coefficients as temperature, temperature based expansion, and burnup. The neutronics runs done include:

- A series of studies to ensure that the external reflectors could provide enough of a reactivity swing to control the reactor over its lifespan. Additionally, the flux profile at the surface of the reactor at different reflector settings was examined.
- A set of calculations to estimate the negative feedback associated with the thermal expansion of the reactor and the Doppler broadening associated with the higher component temperatures.
- A series of runs that simulated some of the credible worst case accident scenarios.
- Two variations on the main cores to fulfill slightly different requirements.
- Other runs to ensure the accuracy of the results and confirm that the core was operating as expected. These include runs using different seeds for the random number generator to ensure that the sampling of the core for the neutrons is sufficient and runs examining the spectrum of the neutrons causing fission in the core in accident cases.
- Additionally, a study to determine the effect of the Nb1Zr cladding on the neutronics of the system.

## **5.1 Initial Calculations**

This section will cover some simple calculations related to the reactor. The reactor had a cold, beginning of life, neutron multiplication factor of  $1.037 \pm 0.001$ , which corresponds to an excess positive reactivity of  $\$5.7$  based on a delayed neutron fraction of 0.0065. The burnup for the reactor was determined using a fairly simple set of equations. The consumption over 10 years at a power level of 200 kWth was 0.8 kgs of  $^{235}\text{U}$  and at 400 kWth, 1.6 kgs of  $^{235}\text{U}$  would be consumed. Given that the fuel loading is 186 kgs of  $^{235}\text{U}$ , the burnup is  $\sim 0.86\%$  for the upper end of the uranium consumed. This burnup results in a loss of  $\$1$  reactivity.

## **5.2 Reactor Multiplication Vs Reflector Position**

The primary goal of this study was to ensure that there was sufficient excess reactivity in the neutron multiplication factor to keep the reactor critical for the 10 year lifespan while ensuring that the reactor would be subcritical during major accident scenarios. The position of the reflector can be used to set the multiplication factor of the reactor. Burnup in the reactor causes a proliferation of additional materials to absorb neutrons and reduces the density of fissile materials, lowering the neutron multiplication of the reactor. This can be offset by closing the reflector, which decreases the neutron leakage of the system. This is shown in Figure 5-1.

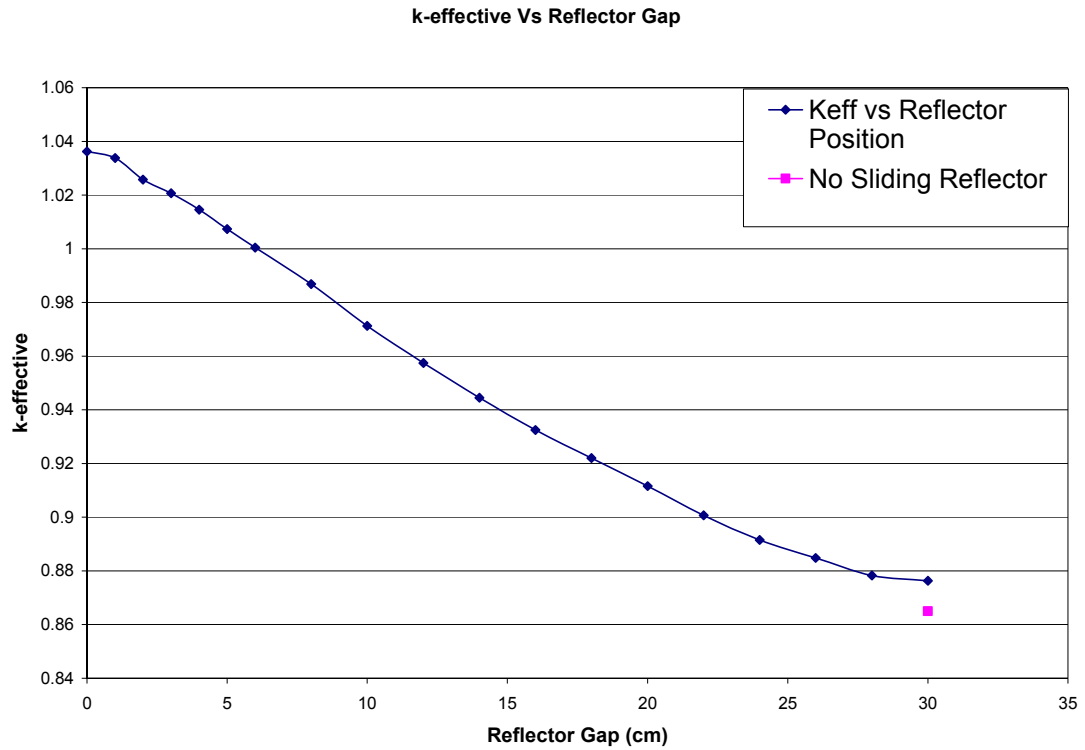


**Figure 5-1 k-Effective Vs Reflector Gap**

The change in neutron multiplication vs reflector position is nearly linear for an extended region. Beyond 22 cm it starts curving, asymptotically approaching the neutron multiplication factor of the core without reflectors. The combined worth of the moveable reflectors is roughly \$26.5 from full open to full closed position. Figure 5-2 shows how the reflectors open up on the core and where the centerline of the reactor is. It also indicates the length of the reflectors.

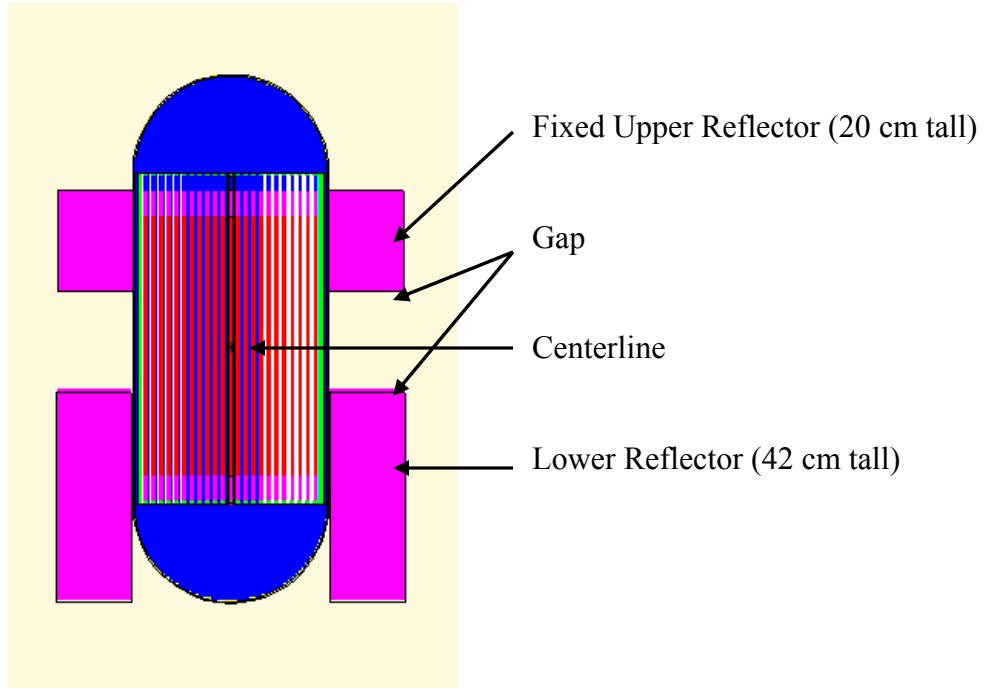


**Figure 5-2 Reflector Movement**

Figure 5-3 shows the results of a series of neutron flux tallies in the pressure vessel. The pressure vessel was segmented into eight different axial pieces of equal size. The plot shows that the axial flux of the reactor is symmetric when the reflectors are closed. As the reflectors open up, the gap causes a distortion in the flux especially adjacent to the gap. This is in line with what would be expected for the reactor.

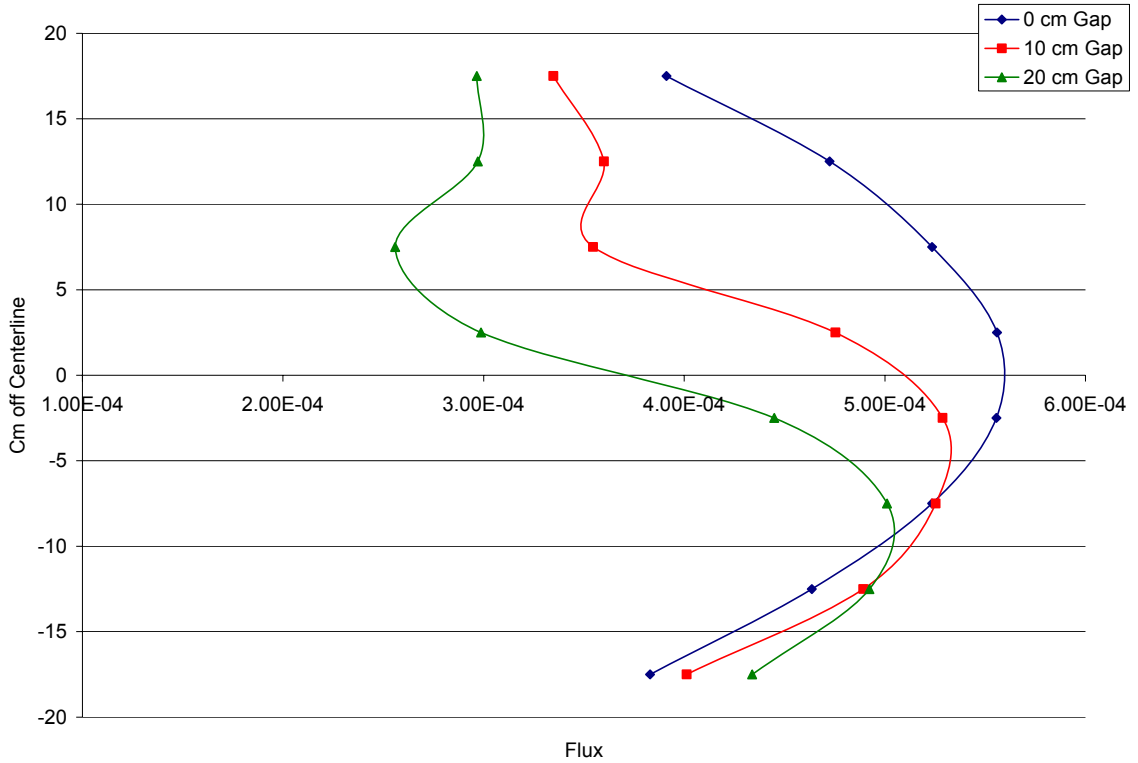


**Figure 5-3 Flux Profile Vs Position for 3 different reflector positions**

### **5.3 High Temperature Feedback effects:**

Most of the calculations run use room temperature cross sections and room temperature dimensions as this is standard practice for determining the rough dimensions and geometry of the core. These runs neglect the effect on cross sections resulting from the increasing temperature, and they also ignore the effects of elevated temperature on the dimensions of the reactors. The cumulative effect of both is investigated in this section. The temperatures used in this section for determining the expansion of reactor components came from an unpublished code, Fission Electric Power SIMulation (FEPSIM) [Lipinski, 2002]. These temperatures are shown in Table 5-1.

**Table 5-1 Temperature Profile of Reactor**

	Temperature (K)
*Fuel Peak	1305
*BeO Axial Peak	1300
*Rhenium	1291.6
*Clad	1291.6
Gas Inlet	850
Gas Avg	1000
*Gas Peak	1144
*Matrix Peak	1217.8
Matrix Edge	960
*PV	860
*Beo Radial	860

\* indicates temperatures used

The assumption is that once the feedback associated with temperature is known the negative feedback coefficient for the reactor can be estimated. This will determine if sufficient excess reactivity is present for the desired mission lifetime. The dimensions of the reactor when heated to the operating temperatures of 1300 K for peak fuel temperature and 860 K in the pressure vessel are shown in Table 5-2:

**Table 5-2 Temperature Adjusted Dimensions of the Reactor**

	Old Radii/Height	New Radii/Height	Change in Thickness
UN/BeO Radial	0.454	0.4591	0.00510
GasGap1	0.46	0.465	-0.00010
Rhenium	0.522	0.5272	0.00020
GasGap2	0.526	0.5311	-0.00010

Cladding	0.57	0.5755	0.00040
Flow	0.735	0.7392	-0.00130
Cell	0.774	0.778	N/A
UN Height	52	52.583	0.58300
BeO Height	5	5.058	0.05800
Gas Plenum	3	3	0.0
Cap	0.5	0.5	0.0
Height	66	66.699	0.69900
Core Radius	19.65	19.77	0.0

One of the conditions imposed was that the cross sectional area of the gas flow gaps would not increase. This was a simplification and as the outer radius of the fuel moved outward to preserve area, the outer radius of the gas gaps expanded slower, resulting in a net decrease in thickness. Note that the change in thickness expressed in the third column does not take into account movement outward caused by expansion of interior components. The cladding is an excellent example of this; its outer radius expands from 0.57 cm to 0.5755 cm, a 0.0055 cm movement. But the bulk of that expansion occurred in the fuel itself and only a tiny fraction (.0003) was a result of expansion of the Nb1Zr cladding. Additionally, the expansion of the hexagonal cells that the fuel pins are suspended in was a more complicated calculation; the ‘radius’ listed is really the ½ pitch between the pins. Slight increases in the thickness at that point results in larger increases in volume than would be the case for cylinders. The expansion of the core radius was a matter of taking the new size of the unit cell and applying it across the centerline of the

core. Since there were 23 pins across the core on the center plane, the radius was increased by that expansion amount. The densities of the materials in the core were also altered to compensate for their increased volume. This was done using a simple Volume (old) to Volume (new) ratio with the results are shown in Table 5-3:

**Table 5-3 Temperature Adjusted Material Densities**

	Vol Ratio	Old Density	New Density
		g/cc	g/cc
UN	0.967	13.924	13.47
BeO	0.978	2.859	2.80
Nb1Zr	0.971	8.59	8.34
Re	0.973	21	20.43

This ensures that while the volumes of components in the core are changing, the mass of each material remains constant. Finally, the cross sections of the materials being used in the core were corrected to those at operating temperature. The vast majority of the materials in the core do not have readily available cross sections at the desired temperature. The NJoy code was used to generate cross sections for the different materials in the reactor [MacFarlane, 1994]. The temperatures used were the peak values from the FEPSIM model. These temperatures are probably somewhat high, but are a much better approximation than using room temperature cross sections. This run resulted in a k-effective of  $1.022 \pm 0.001$ . The net reactivity swing of the system was  $\sim \$2$ . With a total excess reactivity of  $\$5.7$  this leaves another  $\$3.7$  for burnup and other losses.

#### **5.4 Accident Scenarios:**

National expectations for reactors require that any system that would be launched into orbit should not pose a significant risk to the environment or the public in case of a launch accident [DOE, 1982]. Generally this requirement is interpreted to mean that the reactor being designed cannot go critical for any credible accident scenario. Ideally, under accident conditions, the safety margin would be large enough to allow for things to go worse than expected and still be safe. The reactor will be examined for three major accident scenarios: immersion in water, immersion in water with flooding of the core, and immersion in wet sand with flooding of the core. These three accidents represent the credible worst case scenarios commonly examined for space reactor proposals. For these accidents, the design goal is for the reactor to maintain a multiplication factor of less than 0.985.

Increasing the thickness of both the rhenium liner and the uranium nitride pin were required in the reactor design to meet the safety conditions. During normal operations the rhenium had a negative effect on the k-effective but was countered by the extra fuel in the core. In two of the three accident scenarios, the neutron spectrum is more thermal than during normal operation due to the addition of water to the core. For the dry sand accident case, the spectrum is faster than the normal operation case. For the accident scenarios, the extra thermal absorption of neutrons from the additional rhenium dominated the effects from the additional fissionable fuel.

### 5.4.1 Immersion in Water

In this scenario the reactor is immersed in water, and the gas flow region is flooded. It is assumed that the radial reflectors are all removed by any splashdown into water. This scenario results in the moderation of the fast neutrons and normally the increase in cross section with decreased neutron energy would result in an increase in reactivity. The inclusion of rhenium in the core between the fuel and the Nb1Zr cladding negates this effect, as it is a Spectral Shift Absorber. SSA's are materials that are relatively transparent to neutrons in the fast spectrum but a massive absorber at the lower end of the energy spectrum [King, 2005].

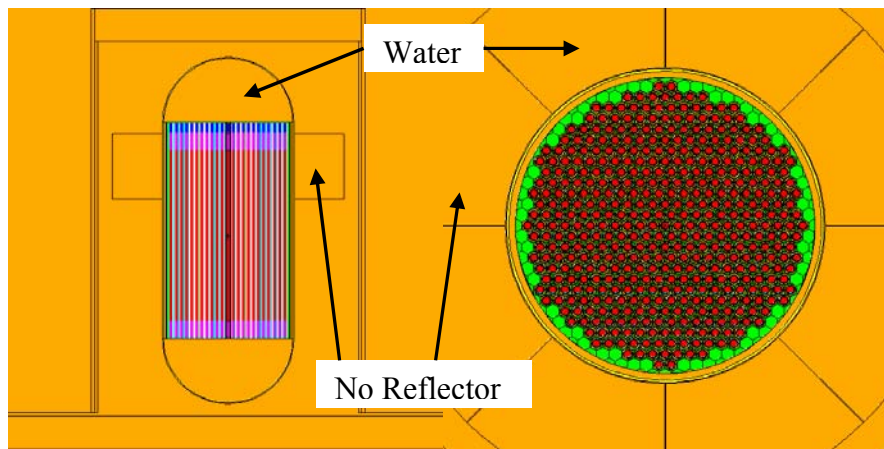


**Figure 5-4 Water Immersion Accident Scenario**

The neutron multiplication factor ( $k$ -effective) was  $0.964 \pm 0.001$ , well below the desired value of 0.985.

### 5.4.2 Immersion in Wet Sand with Water Flooding

In this scenario the core was immersed in wet sand (70% sand by volume, 1.924 g/cc) with the core flooded with water. This accident scenario includes a variety of negative aspects: the water is moderating the neutrons to a significant degree, and the sand is an

excellent reflector. This accident scenario has often been a more challenging one than the water immersion case.

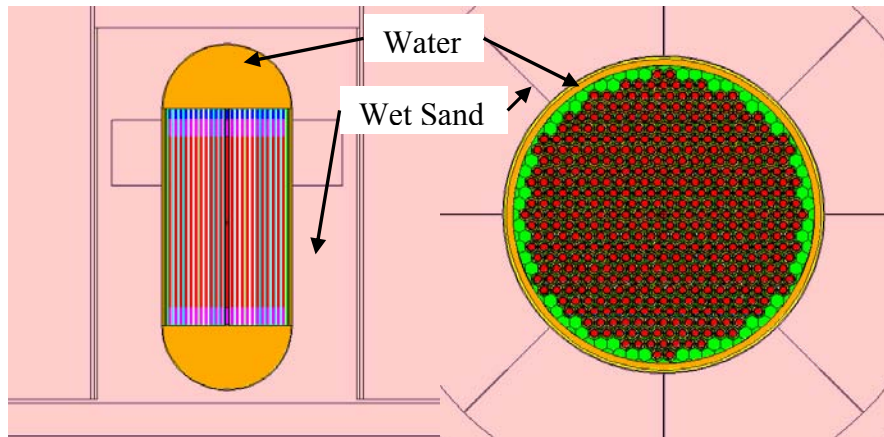


**Figure 5-5 Wet Sand, Water Scenario**

For this case the k-effective was  $0.975 \pm 0.001$ ; much closer to the margin of 0.985

### **5.4.3 Dry Sand Burial**

This accident scenario involved the reactor being buried in SiO<sub>2</sub> with a density of 1.5 g/cc. This is a median point between the density of loose sand (1.4 g/cc) and dry, packed sand (1.6 g/cc). The core is not flooded in this case, and the radial reflectors have been removed. While little moderation occurred in the sand and SiO<sub>2</sub> is an inferior scattering medium to BeO (and is also without the (n,2n) reaction), the reactor was going from somewhat reflected to essentially infinite reflection conditions. In a variety of cores this had led to a net increase in reactivity. This effect is highly dependent on the density of the sand. This core had a k-effective of  $0.981 \pm 0.001$  for this scenario.

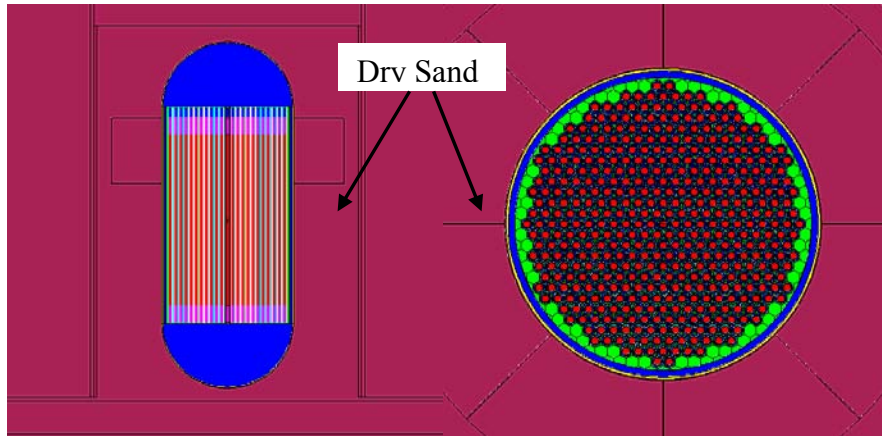


**Figure 5-6 Sand Burial Accident Scenario**

The results from these runs can be found in table 5-3

**Table 5-4 Accident Scenario Results**

<b>Accident Conditions</b>	<b>K-Effective</b>
Full Water Immersion, Flooded, No Reflector	0.96387 ±0.001
Full Wet Sand Immersion, Flooded, No Reflector	0.97484 ±0.001
Full Dry Sand Immersion, No Reflector	0.98101 ±0.001

These results show that the reactor is substantially subcritical in all of these accident scenarios. The most problematic of the accident cases is the dry sand immersion case, which is also the least credible of the accident scenarios. The likelihood of a reactor coming down intact and burying itself in sand is low. At high velocities even water starts

looking like concrete on impact. None of these scenarios included modeling of deformation of the reactor core.

### **5.5 Alternative Cores:**

Two major variations on the primary core were analyzed. One core was a test bed reactor that would use low enrichment fuel of roughly similar dimensions in a thermal assembly to simulate some of the effects of the reactor while still falling below the category III threshold. The Category-III threshold is less than 6 kg of  $^{235}\text{U}$  at any enrichment, or it can be less than 50 kg of  $^{235}\text{U}$  at an atom enrichment of less than 50%. This will reduce the security costs relating to the reactor. The other core places a boron carbide cylinder along the centerline of the reactor to provide an additional safety margin during the launch of the reactor.

#### **5.5.1 Category-III Reactor**

Significant cost savings in security and development can be had if the reactor uses a Category-III level of SNM rather than Category I. Security for facilities with highly enriched fuel on site can cost roughly \$30 M per year and the slow down in experimental operations caused by this security can cause an additional cost. The first option requires a well-moderated reactor; the second requires a somewhat moderated reactor. The first option may end up being very limited in power and lifetime because of fuel burnup; the second option has more latitude for power and burnup.

A Category-III space reactor was not designed for this study. But consideration was made for a Category-III reactor that would simulate the behavior of a Category-I space reactor. The intent would be to make preliminary nuclear-heated ground tests less

expensive. There are drawbacks however. The similarity between the test reactor and the final design would be somewhat limited. Thus far, the Category III core has not proven safe for the common launch accident scenarios. The two alternatives that have been examined are listed below.

One possible design uses pins that are at the upper limits of category III definition (49%, 49kg  $^{235}\text{U}$ ) to achieve the desired results. In this case, the size of the fuel pins would have to be reduced or the number of pins would have to be reduced. Specifics of this core will be covered in the first alternative core. Another method for achieving the desired results is to use a lower enrichment fuel and maintain the fuel pin geometry of the original Category I reactor as much as possible. This design will be detailed in the second alternative core description. Both of the designs share many similarities; particularly that the reduced  $^{235}\text{U}$  enrichment requires the reactors to be thermal systems, which limits the usefulness of comparison between the space reactor and the test-bed. The changeover to a thermal system requires the use of a high temperature moderator. The primary material being investigated is yttrium hydride. Yttrium hydride appears to be a stable high-temperature moderator, though data on its materials and neutronics characteristics is limited. Yttrium Hydride would replace the Nb1Zr matrix between the fuel pins in the original designs and would likely have a cladding of some material to minimize hydrogen leakage. In these runs, a generic stainless steel was used to estimate the neutronic impact of such a liner; a more temperature appropriate choice will have to be made. To get sufficient moderation the pitch of the reactor will increase significantly when compared to the original core.

### 5.5.1.1 Alternative 1 Reactor

This section covers the Reactor that uses 49% enriched  $^{235}\text{U}$ , 49 kg fuel. The Alternative 1 reactor uses smaller radius fuel pins enriched to 49% and was the simpler of the two cores to achieve a supercritical configuration with. The active length of the older source core was retained, the cross sectional flow area increased, and the overall core radius decreased. Cross sectional screenshots of the design are shown in Figure 5-7 through Figure 5-9.

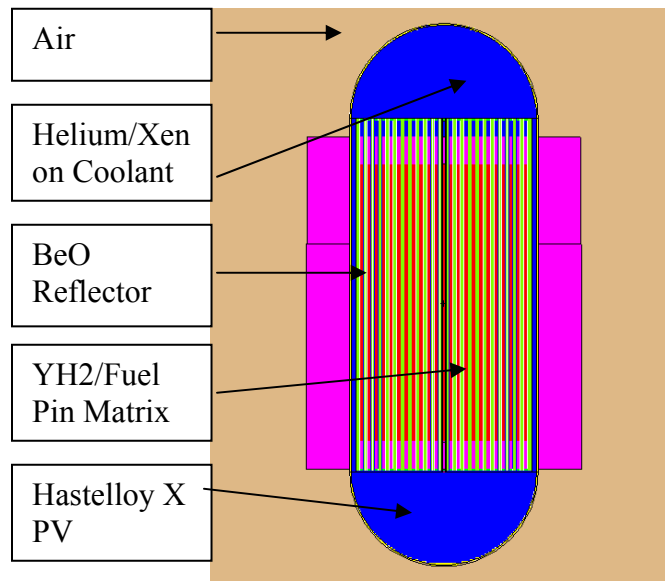


**Figure 5-7: XZ Plane Section of Reactor Alternative 1**

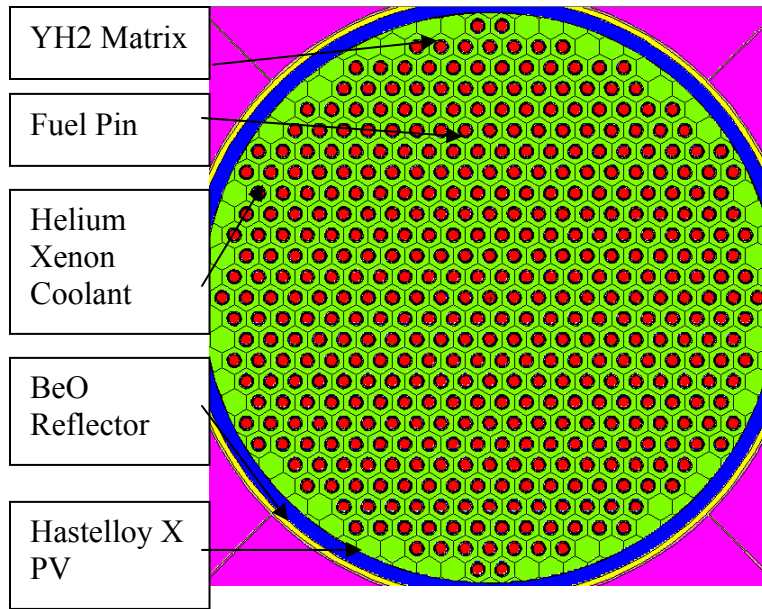


**Figure 5-8 XY Cross Section of Reactor Alternative 1**

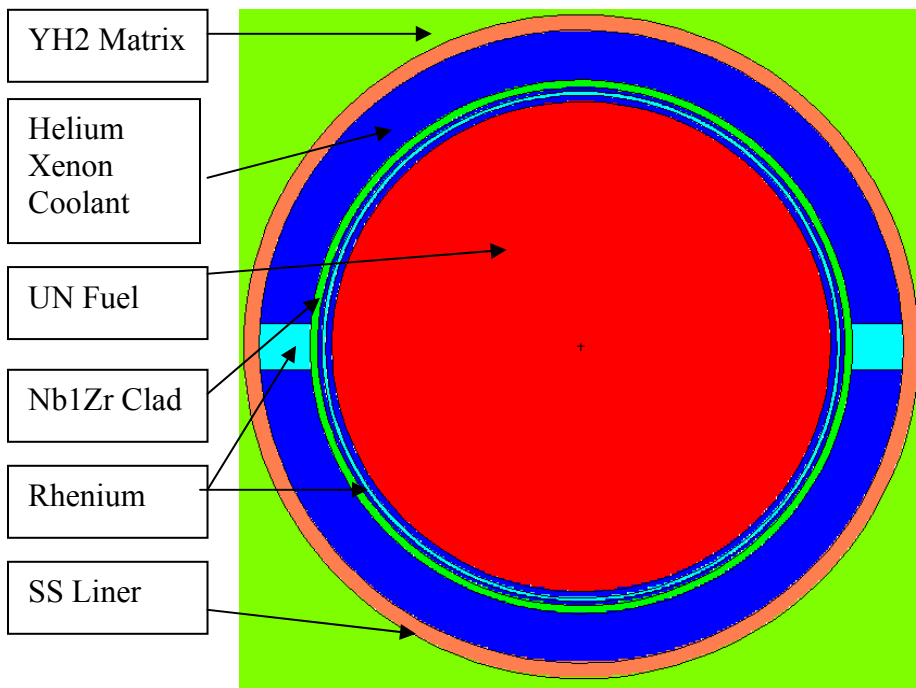


**Figure 5-9 Close up of XY plane, Alternative 1 Reactor**

A further parameter search increasing the pitch between the fuel pins and placing extra yttrium hydride in the matrix was done. The effect of pitch on k-effective is shown in

Figure 5-10. It shows that the minimum dimensions design was nowhere near the optimally moderated case and that there was a great deal of margin available for achieving criticality if needed.

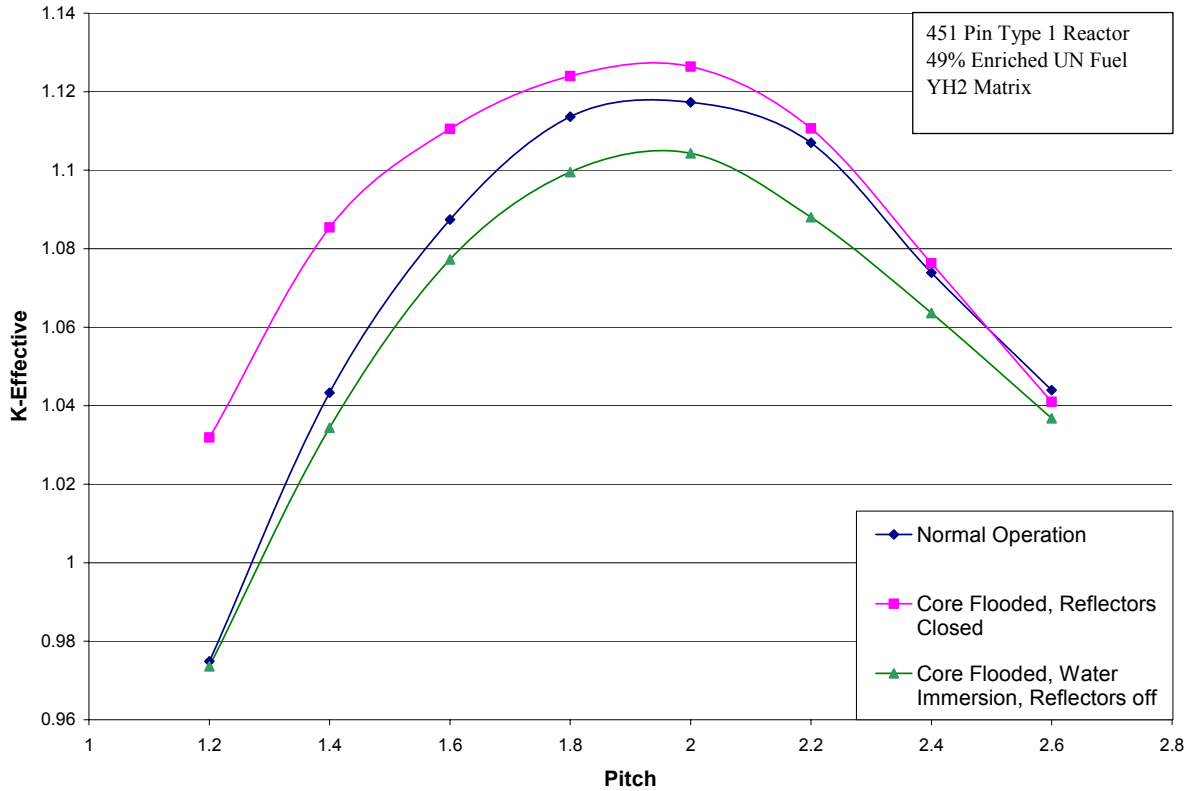


**Figure 5-10 K-Effective Vs Pitch, Alternative 1 Core**

Some downsides to this design are inherent in the decision to go with a thermal system. Several of the launch accident scenarios provide an unacceptable risk of the core going supercritical. Any scenario where water or additional moderator enters the core is likely to result in a supercritical configuration. This largely was the result of the need to decrease the thickness of the rhenium layer in the fuel to allow for a critical thermal system, and thus is probably unavoidable.

### **5.5.1.2 Alternative 2 Reactor**

The Alternative 2 reactor is an attempt at designing a lower enrichment reactor that will fulfill the requirements of a Category III reactor while allowing for a greater degree of similarity with the source reactor than the above Alternative 1 design. To ensure this similarity the radial dimensions of the uranium nitride fuel is the same as the Category 1 reactor source, but the fuel length, enrichment, pitch, and the number of fuel pins were all varied. When the fuel length was reduced the fuel was replaced with additional BeO reflector. The gas flow gap was held fixed. This meant that the flow channels for the gas are the same as those in the original design. Another change that was necessary was a slight reduction in the thickness of the rhenium layer between the UN fuel and the Nb1Ze clad from .1mm to .07mm. This reduced the losses in the rhenium due to thermal neutron absorption. The substitution of yttrium hydride for the Hastelloy increases the radius of the core significantly. The first core that was critical employed a combination of the variables listed to achieve criticality: 397 fuel pins, 40cm fuel length, and 39% enriched fuel. There are probably a variety of ways to achieve the desired results; this was the first combination that met the requirements. Achieving the desired results only using 2 of the 3 primary variables (active length and pitch) has proven difficult. An alternative that retains the original active length and pitch, but reducing the number of pins and increasing the enrichment might be viable and worth investigating. Figure 5-11 through Figure 5-123 show a series of cross sectional slices of the core.

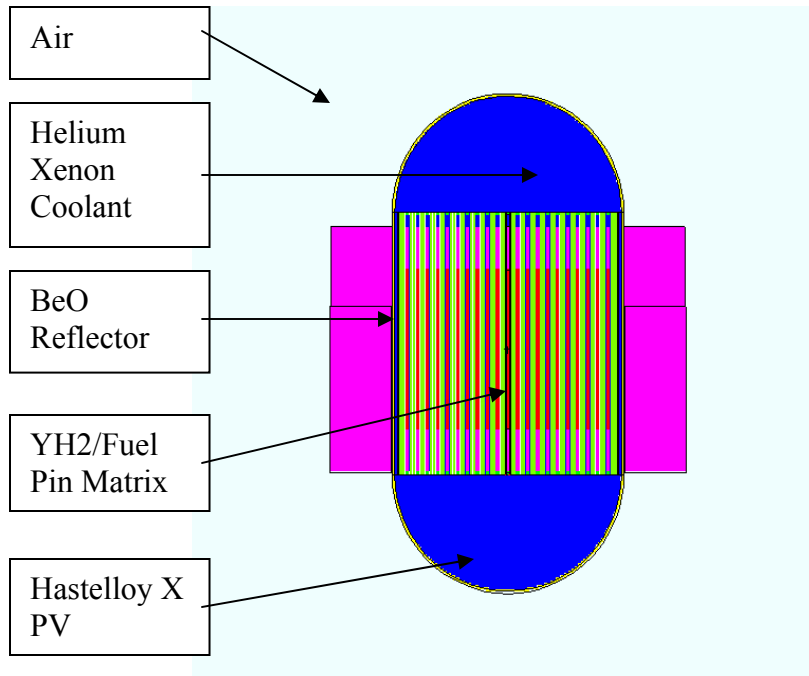


**Figure 5-11 XZ Cross Section of Alternative 2 Reactor**

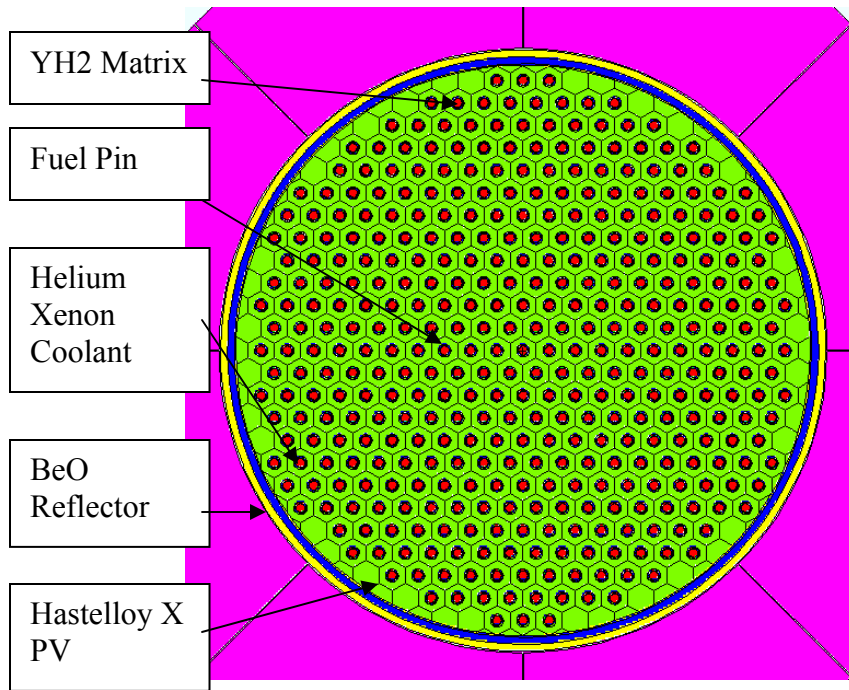


**Figure 5-12 XY Cross Section of Alternative 2 Reactor**

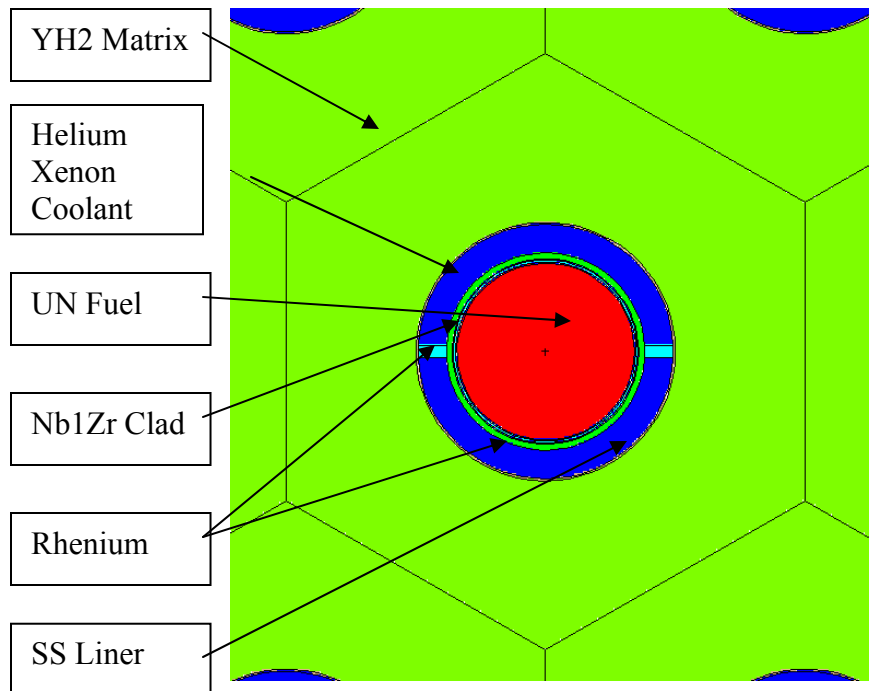


**Figure 5-13 Close up of XY Plane, Alternative 2 Reactor**

### **5.5.2 Boron Carbide Central Safety Rod**

The ability to launch a reactor into orbit with a negligible chance of accidental criticality is one of the keys to having a successful program. Other work has indicated that dropping the reactor on to an unyielding surface could cause the reactor to become critical as the fuel pins deformed [Lenard, ]. Some runs for a gas-cooled reactor indicated that if compression caused a reduction in the pitch of the fuel pins the core could also become critical. Several ways of mitigating the impact on the system were investigated. Placing a large rod of polyethylene with a thin layer of boron carbide was a fairly effective way of mitigating the impact. Figure 5-14 and 5-15 show two slices of the core that illustrate the differences quite well.

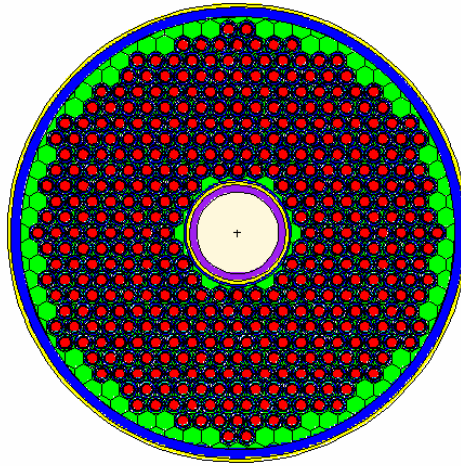


**Figure 5-14 XY Plane Section of Internal Control Rod Reactor**

This XY plane section shows the safety rod inserted in the center of the reactor.

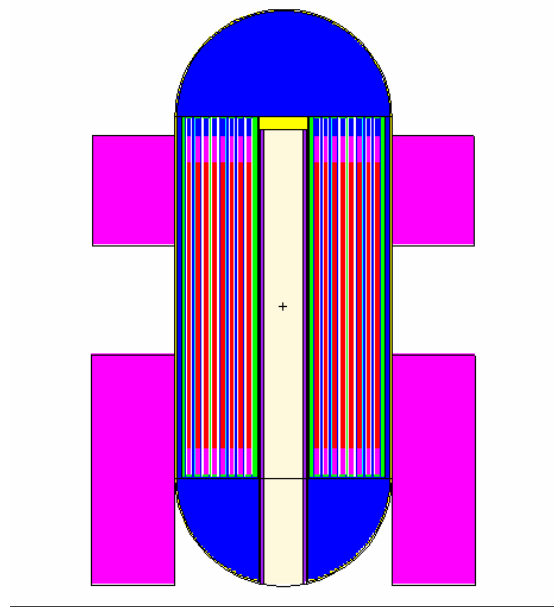


**Figure 5-15 XZ Plane Section of Internal Control Rod Reactor**

Figure 5-15 shows an XZ cross sectional slice of the reactor. The B4C rod displaces 37 fuel pins from the center of the core but 36 of these are added back to the outer ring of fuel pins with minimal impact on the size of the core. With the rod in place and the reflectors closed the multiplication factor is 0.993. This is close to the case without the control rod because of the transparency of materials at high neutron energies. During water immersion accident scenarios the rod results in a significant decrease in excess reactivity  $.940 \pm 0.002$ . Without the rod and with the reflectors closed the multiplication factor is  $1.005 \pm 0.001$ , well below what was seen in the original design. Additional fuel would have to be added to make this core practical. These changes complicate the design significantly. To avoid the problems of welding dissimilar materials the ‘thimble’ for the control rod has to be made of the same material as the pressure vessel but its placement along the centerline of the core increases the radiation flux it sees and the temperature at that location. Neither of these things are good as HastX was a marginal choice in the first place at the temperatures at outer surface of the cylinder. Either a material that can be reliably welded to HastX has to be found or the thimble needs to be cooled.

Table 5-5 shows details all of the designs.

**Table 5-5 Reactor Dimensions and Compositions**

<b>Core</b>	<b>Primary Design</b>	<b>Alternative 1</b>	<b>Alternative 2</b>	<b>B4C Rod</b>
<b>Gas Properties</b>				
Coolant	He/Xe	He/Xe	He/Xe	He/Xe
He fraction	<b>70/30</b>	<b>70/30</b>	<b>70/30</b>	<b>70/30</b>
Total Mass (kg)	<b>1073</b>	<b>910</b>	<b>1789</b>	<b>1070</b>
Mass U235	<b>186</b>	<b>49</b>	<b>49</b>	<b>185</b>

<b>Reactor Core, Vessel, Reflectors</b>				
Type	Pin-matrix	Pin-matrix	Pin-matrix	Pin-matrix
Reactor Material Properties				
Fuel material	UN	UN	UN	UN
Clad material	Nb1%Zr	Nb1%Zr	Nb1%Zr	Nb1%Zr
Clad liner material	Re	Re	Re	Re
Wire wrap material	Re	Re	Re	Re
Moderator material	N/A	YH <sub>2</sub>	YH <sub>2</sub>	N/A
Matrix (core block) material	Nb1%Zr	YH <sub>2</sub>	YH <sub>2</sub>	Nb1%Zr
Matrix wall material		SS304	SS304	N/A
Pressure vessel material	HastX	HastX	HastX	HastX
Radial reflector material	BeO	BeO	BeO	BeO
Axial reflector material	BeO	BeO	BeO	BeO
Lower grid material	Nb1%Zr	HastX	HastX	Nb1%Zr
Upper grid material	Nb1%Zr	HastX	HastX	Nb1%Zr
Coolant material	He/Xe	He/Xe	He/Xe	He/Xe
Fissile material	U-235	U-235	U-235	U-235
Fuel enrichment	<b>0.9315</b>	<b>0.4899</b>	<b>0.3789</b>	<b>0.9315</b>
Reactor Radial Dimensions				
Radius of the fuel (UN only) (m)	<b>4.54E-03</b>	<b>3.21E-03</b>	<b>4.44E-03</b>	<b>4.54E-03</b>
Thickness of the fuel gap (m)	<b>6E-05</b>	<b>5E-05</b>	<b>7E-05</b>	<b>6E-05</b>
Thickness of the liner (m)	<b>6.2E-04</b>	<b>5E-05</b>	<b>1E-04</b>	<b>6.2E-04</b>
Thickness of liner- clad gap (m)	<b>4E-05</b>	<b>5E-05</b>	<b>6E-05</b>	<b>4E-05</b>
Thickness of the clad (m)	<b>4.4E-04</b>	<b>1E-04</b>	<b>3E-04</b>	<b>4.4E-04</b>

Thickness of coolant channel (m)	<b>1.65E-03</b>	<b>1.64E-03</b>	<b>1.43E-03</b>	<b>1.65E-03</b>
Width to thickness ratio of rectangular wire	1	1	1	1
Pitch of the wire wrap (m)	0.2	0.2	0.2	0.2
Number of wires wraps per pin	2	2	2	2
Thickness of matrix between pins (m)	<b>7.8E-4</b>	<b>1.14E-02</b>	<b>1.3E-02</b>	<b>7.8E-4</b>
Number of fuel pins	<b>451</b>	<b>451</b>	<b>397</b>	<b>450</b>
Thickness added to circle to get matrix radius (m)	0.016	0.016	0.016	0.016
Thickness of matrix insulation (He/Xe) (m)	0.0002	0.0002	0.0002	0.0002
Thickness of the matrix & dome baffle (m)	1E-06	1E-06	1E-06	1E-06
Thickness of the downcomer channel (m)	0.008	0.008	0.008	0.008
Thickness of the pressure vessel (m)	0.003	0.003	0.007	0.003
Thickness of the reflector gap (m)	0.001	0.001	0.001	0.001
Thickness of the radial reflector w/o clad (m)	0.15	0.09	0.16	0.15
Reactor Axial Dimensions				
Length of the active fuel in the reactor (m)	0.52	0.52	0.40	0.52
Length of the axial fuel plenum (m)	0.03	0.03	0.03	0.03
Length of upper axial reflector (m)	0.05	0.05	0.11	0.05
Length of lower axial reflector (m)	0.05	0.05	0.11	0.05

Length of each end cap (m)	0.005	0.005	0.005	0.005
Length of the lower grid plate & pin flow orifices (m)	N/A	N/A	N/A	N/A
Length of the outlet (upper) plenum (m)	0.005	0.005	0.005	0.005
Length of the inlet (lower) plenum (m)	0.005	0.005	0.005	0.005
Other				
Axial peak-to-avg ratio in core	1.2	1.2	1.2	1.2
Radial peak-to-avg pin power	1.2	1.2	1.2	1.2
SiO <sub>2</sub> fraction in wet sand	0.64	0.64	0.64	0.64
K-Effective of Core	<b>1.037 ±0.001</b>	<b>1.0758 ±0.001</b>	<b>1.004 ±0.001</b>	<b>1.005 ±0.001</b>

### 5.6 Quality Control Runs

The following results represent an effort to better understand how the reactor would operate and to increase confidence in the proposed design. The first of these runs ensures that the neutron population was adequately sampled. A series of runs using a different seed for the random number generator should generate a distribution of results. If 2/3 of the runs are within one sigma of the average, then it is likely that the model is being adequately sampled. If not, there are a variety of possible reasons for the problem. One possibility is that insufficient particles are being or a significant portion of the core is being ignored. This can work in both ways: the sampling happens predominantly in the outer layer of the core, depressing the k-effective or the sampling happens mostly in the center of the core, underestimating leakage. A total of twenty different runs were done for the core and the results are shown in Figure 5-16

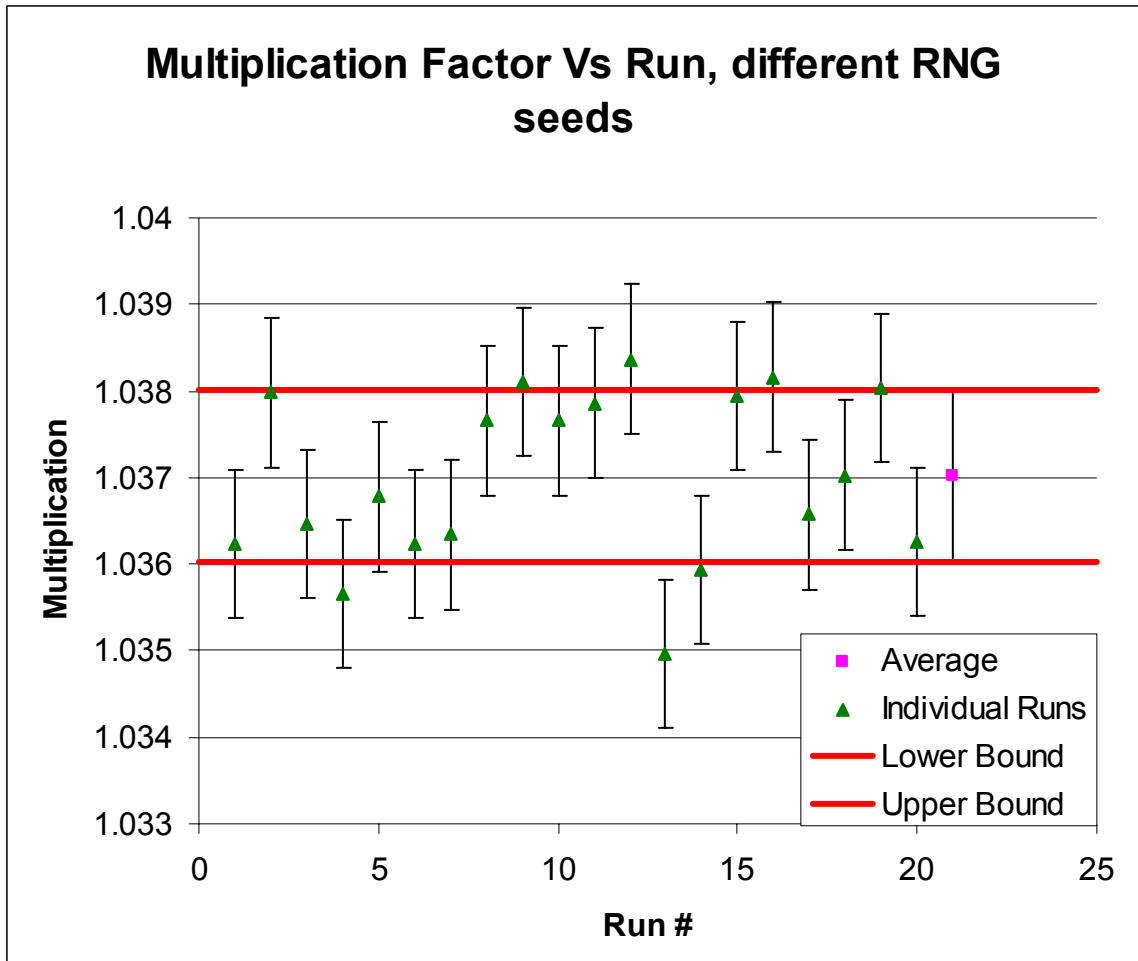


**Figure 5-16 Multiplication vs. Run with different RNG seeds**

The runs show that between 6 and 7 of the 20 runs done fall outside the one sigma deviation, exactly what would be expected. This give an average multiplication factor of  $1.037 \pm 0.001$ . The second set of runs was focused on what the spectrum of the neutrons causing fissions in the reactor during accident cases. The results are shown in Figure 5-17

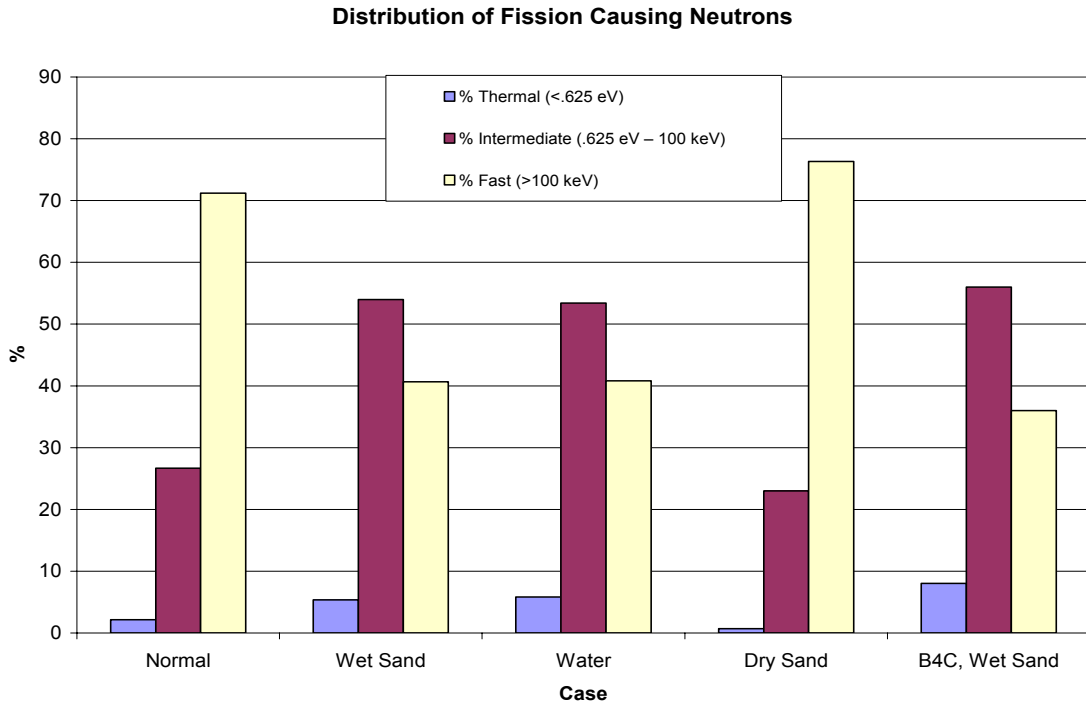


**Figure 5-17 Distribution of Fission Causing Neutrons**

During normal operation the vast majority of fissions are caused by fast or intermediate energy neutrons, which is what one would expect in a slightly moderated core. During the accident case where water gets into the core, the distribution of the fission causing neutrons swings heavily towards the intermediate range with the thermal range neutrons showing a significant increase. The dry sand accident scenario shows the opposite: the spectrum of the neutrons causing fission actually gets somewhat faster. Finally, the case with a B4C control rod and wet sand immersion looks similar to the normal wet sand case, but with a more thermalized distribution.

Another series of runs were done to determine the effect of the Nb1Zr cladding on the neutronics of the system. One of the reasons for doing these runs was the possibility that Nb1Zr might end up being incompatible with the UN fuel and there was a desire to

know how large a part it played in determining the neutron multiplication factor of the core. The runs took a single fuel hexagon and put reflective boundaries around it. This effectively made the core an infinite system. Removing the cladding increased the k-effective of the system by 0.0056, or 0.86\$. This was with the standard deviation being much smaller than the neutron multiplication factor swing, averaging 0.001. Thus, there is a sufficient margin that if an alternative cladding to become a necessary, it would not require massive reworking of the core to incorporate it.

## 6 Thermal Evaluation of Core and Remainder of System

Neutronics effects were not the only aspect of the system to be examined for this design. A basic evaluation of the properties related to the power conversion system was also done. The Fission Electric Power SIMulation spreadsheet set was used for thermal analysis in a variety of ways [Lipinski, 2002]. Its inputs included an approximation of the reactor core dimensions used in MCNP, dimensions and materials composition for the remainder of the system (radiator, piping, etc) and inlet temperatures for the turbine. FEPSIM takes this information and estimates, among other things, the peak fuel, liner, cladding, and pressure vessel temperatures. This allowed the expanded dimensions of the different components at operating temperature to be determined and used in later MCNP runs. The efficiency of the power conversion system and whether the pressure losses were severe enough to cause the Brayton Cycle to stall were also generated.

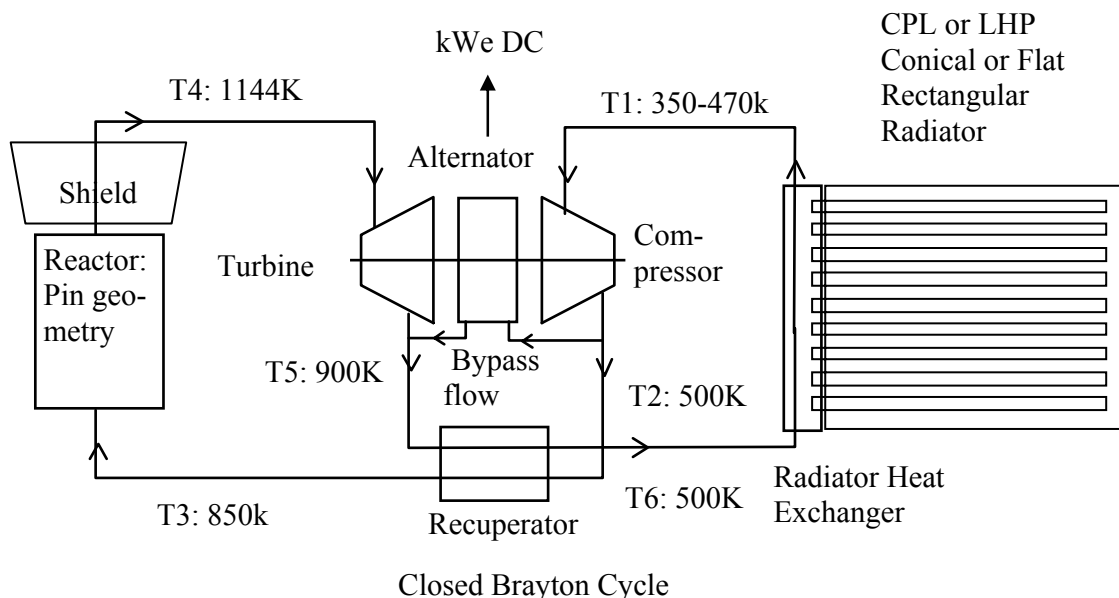


**Figure 6-1 FEPSIM components with State temperatures**

## **6.1 Radiator**

The radiator used in the reactor has a drastic effect on the output power of the reactor. For the models used, the temperature of the gas coming out the reactor is held at a fixed temperature. Gas passing through the turbine has a certain temperature drop. The gas then reaches the radiator which further cools the gas. The amount that the gas is cooled in the radiator is highly dependent on the size of the radiator. This becomes extremely important when determining the amount of work the compressor has to do. At lower temperatures and pressures, the work done by the compressor to compress the gas to the reactor inlet conditions is low. As the temperature increases the amount of work increases, decreasing the net power output.

Initially, the radiator dimensions were carried over from a higher power reactor that had 200 m<sup>2</sup> of radiating area. This was an enormously oversized radiator that resulted in the inlet temperature for the reactor being low and the power conversion efficiency high (as high as 37%). To see what effect radiator parameters could have on the core, 4 different sizes of radiator at 5 different thermal power levels were examined. The radiator areas were, from low to high, 80 m<sup>2</sup>, 98 m<sup>2</sup>, 140 m<sup>2</sup>, and 200 m<sup>2</sup>. The thermal power levels examined were 200 kW, 250 kW, 300 kW, 350 kW, and 400 kW.

Figure

6-2 shows the electric power vs. thermal power for the different radiators.

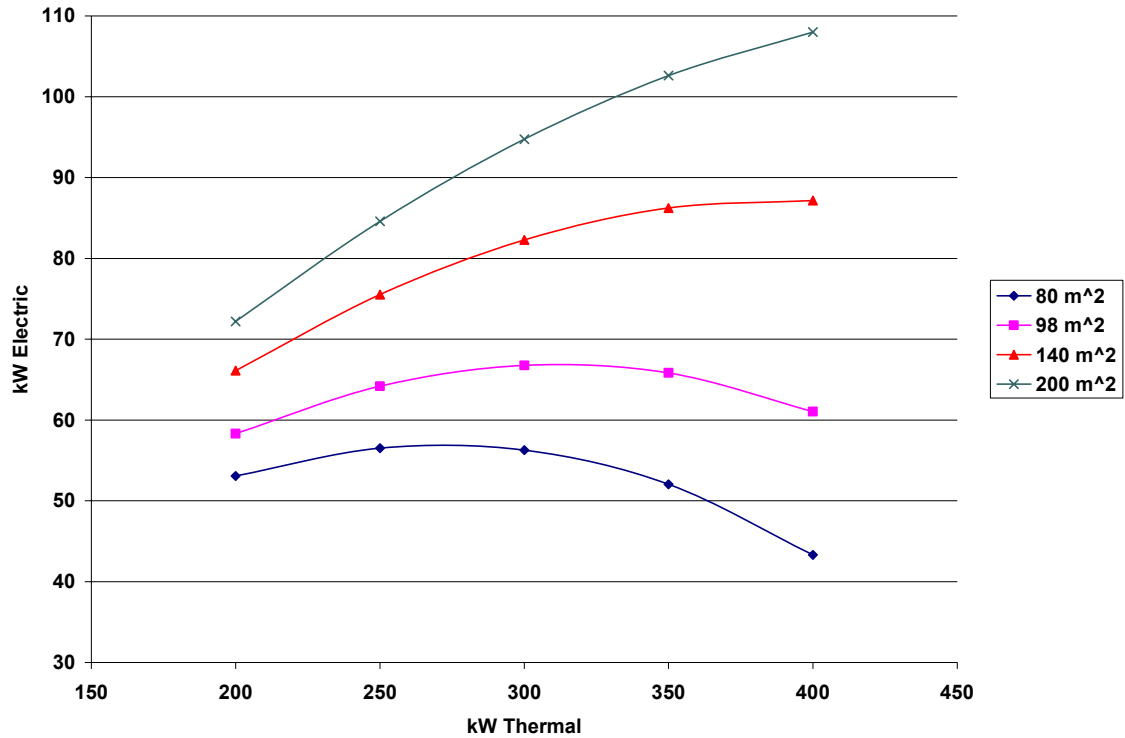


**Figure 6-2 Electric Output vs. Thermal Output**

This plot shows that for the smaller radiators the power output peaks in the range under examination and then starts to drop off. As the thermal power goes up for the designs with the larger radiators the electric power keeps on rising. If these plots were extended to even higher thermal power outputs they would peak also. This is a result of the different rates at which the electric conversion cycle efficiency is changing. This is shown on Figure 6-3

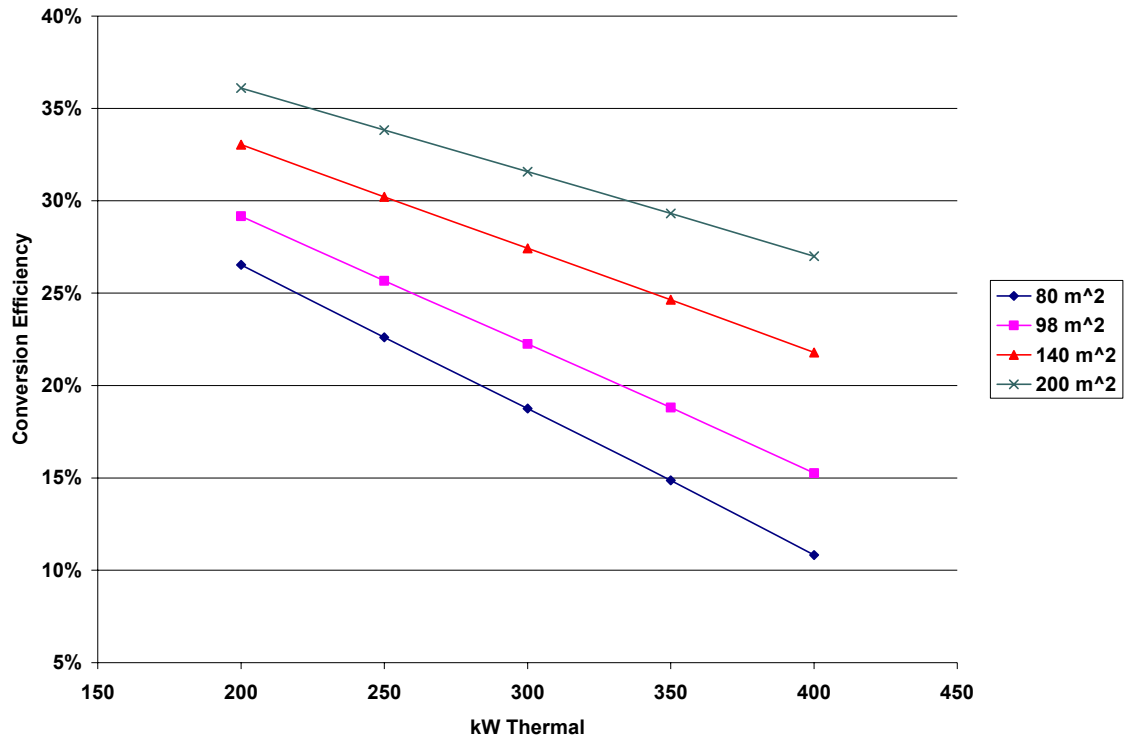


**Figure 6-3 Conversion Efficiency Vs Thermal Output**

The thermal efficiency of all the systems are falling, but at different rates. The smallest radiator drops from 27% efficiency at 200 kWth to 11% efficiency at 400 kWth. This means that in the process of doubling the thermal output of the reactor the conversion efficiency has dropped by more than half, causing a net loss in power output. On the other hand, the 200 m<sup>2</sup> radiator drops from an efficiency of 36% to 27%, a drop of a third, while the thermal power doubles, generating a net increase in power output ( $400 \cdot 0.27 > 200 \cdot 0.36$ ). Finally, the weight of the system needs to be examined. One way of expressing this is the inverse specific power (expressed in estimated system kg /power output) vs. the thermal power of the system. This is shown in 6-4. The density per unit surface area of the radiator was fixed at 5 kg/m<sup>2</sup>

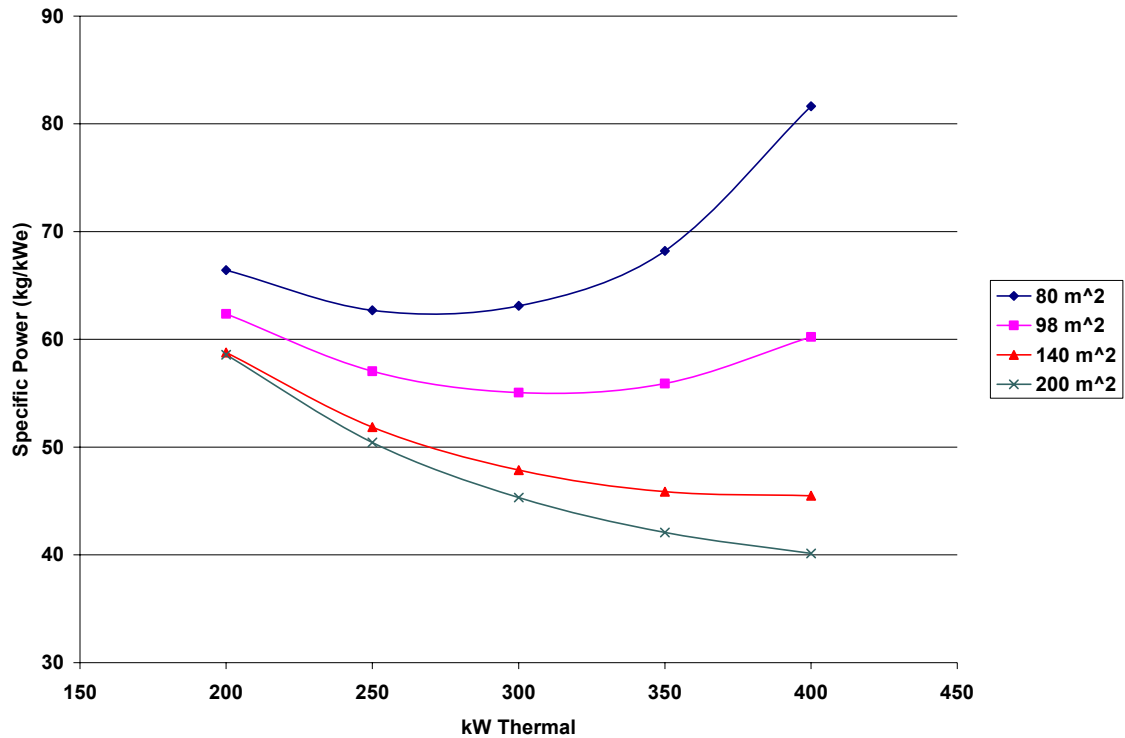


**Figure 6-4 Specific Power Vs Thermal Output**

This implies that larger radiators allow for more mass effective production of power. The only variables are the thermal output and the size (and mass) of the radiator. For the 80 m<sup>2</sup> radiator as the thermal power goes up the efficiency goes down while the weight of the radiator stays the same, so the effectiveness of the system drops. The general result of this is that the size of the radiator one chooses for the reactor depends on several considerations. What is the desired power output? How much margin is to be included to mitigate the effect of system degradation? Is the system intended to be a variable power system operating at a variety of levels or a system that has constant power output? All of these questions need to be answered. All of these Figures show that if the desired output is in the 50-60 kWe range the radiator only needs to be 80-98 m<sup>2</sup>. If higher outputs are desired (greater than 100 kWe range) a larger radiator of about 200m<sup>2</sup> would be needed.

For these designs, the primary fixed property was the turbine inlet temperature.

Variables such as the gas flow rate and the pressure drop was variable. This means that the temperature of the fuel is also variable, so one has to examine that as well to ensure that safety margins have not been violated. These runs show that the power output is more dependent on the size of the radiator than the size of the reactor. Significant increases in power for a given core can be achieved by increasing the size of the radiator..

## 7 Conclusions and Future Work

### 7.1 Conclusions

The primary goal of this thesis was to do design work on a GCR-CBC reactor. The focus was on the neutronics of the core with basic analysis of the other components of the design. There is a significant region where a GCR pin type core looks to be feasible. While materials issues warrant examination, no critical problems were found. A variety of MCNP runs were done covering a wide range of situations and none of them cause a problem that a small amount of tuning of the design could not resolve. The thermal radiation component showed just how complicated a reactor system can be. The tradeoffs between radiator size, electrical output, and thermal efficiency are extremely complicated.

The reactor was to meet some specific requirements. The design was to be a gas-cooled, pin type reactor. This was a fairly easy requirement to meet. The desired power output was 100 kWe. This was more complicated, depending on the efficiencies of the Brayton cycle, the thermal output of the reactor and all the related conditions to ensure that the Brayton cycle was stable. The requirement that the reactor have a 10 year lifespan at full power was easily met given that the fuel was highly enriched. For a thermal neutron spectrum system the lifespan requirement might be more of an issue. Finally, there was to be some investigation into how the reactor would be modified to make it work in a Martian atmosphere. This requirement ended up being a fairly problematic in that it required a great deal of materials engineering knowledge.

For GCR-CBC reactor there is a great deal of interaction between the components and a system wide view is important. It is insufficient for the reactor to be critical: if the

gas flow across the pins generates enough pressure loss to stall the Brayton cycle the system will not work. The power output is highly dependent on the amount of waste heat the radiator can vent. Design of a functional system will require a great deal of interdiscipline collaboration.

## **7.2 Future Work**

There is a great deal of potential work to be done on the reactor design. Materials engineering related problems are one area with a great deal of potential work. Expanding on the limited data on HastX and Nb1Zr compatability is one area that needs work. The amount of oxygen and other contaminants that would be leeched from the Hast-X and how much of these contaminants would diffuse into the Nb1Zr components of the reactor is one of the potential problems. Further testing of HastX in a mars-like atmosphere to characterize its interaction with that environment would also be valuable. Further data on how rhenium and UN interact and what occurs when they are both irradiated are also potential topics. There were some more conventional mechanical engineering problems that were unaddressed. While the strengths of the materials used was examined, the stresses that would be generated were not examined. The pressures generated by the release of fission gasses are one possible problem. Another is stresses generated by the different expansion rates of the materials. Shielding for radiation was not addressed in this thesis. Finally, the design of the Brayton cycle and any optimization that would be related to that part of the reactor was not addressed in this thesis.

## References

Angelo, J. A., Jr., and D. Buden, *Space Nuclear Power*, Orbit Book Company, Inc., Malabar, FA, 1985.

Biaglow, James A., *Rhenium Material Properties*, ASME, SAE, and ASEE, Joint Propulsion Conference and Exhibit, 31st, San Diego, CA, AIAA-1995-2398 July 10-12, 1995.

Brown, Nicholas, *Gas-Cooled Reactor Vessel Design and Optimization with COSMOSFloWorks*, American Nuclear Society Student Conference, Rensselaer Polytechnic Institute, NY, March 31, 2006.

Brown, W.F., et. al., *Aerospace Structural Metals Handbook*, CINDAS/Purdue University, code 4112, 1992 ed.

Davis, J.E., *Design and Fabrication of the Brayton Rotating Unit*, NASA/CR-1870, March 1972.

DiStefano, J. R., Hendricks, J. W., *Oxidation of Nb-1Zr in Space System Environments*, ORNL-TM-11423, Oak Ridge National Laboratory, 1990.

El-Wakil, M. M., *Powerplant Technology*, pp. 309-351 433, 1984.

Furlong, Richard R. *U.S. Space missions using radioisotope power systems*, Nuclear News, April 1999, page 28.

Horak, J. A., *Data Correlations and Creep Equations for Nb-1%Zr and PWC-11*, ORNL Letter 0514/20/85. May 14, 1985.

Johnson, C. E., *Thermophysical and Mechanical Properties of Advanced Carbide and Nitride Fuels.*, ANL-AFP-26., June 1976.

Keiffer, H. H., Jakosky, B. M., Snyder, C. W., and Matthes, M. S. (Editors), *Mars*, Univ. of Arizona Press, Tuscon, AZ, 1992.

King, J.C., El-Genk, M. S., *Spectral Shift Absorbers for Fast Spectrum Space Nuclear Reactors.*, in proceedings of *Space Technology and Applications International Forum (STAIF 2005)*, edited by M. El-Genk, AIP Conference Proceedings 746, New York, 2005.

Lipinski R. J., *FEPSIM*, Sandia Internal Space Reactor Power System Design Code, Unpublished, 2002.

MacFarlane, R.E., Muir, D. W., *The NJOY Nuclear Data Processing System Version 91*, LA-12740-M, October 1994.

*Niobium Metallurgical Products*,  
<http://www.dhcommunications.com/success/shared/niobium%20brochure.pdf>, accessed March 15, 2006.

*NIST Chemistry WebBook* <http://webbook.nist.gov/chemistry/> accessed March 1<sup>st</sup>, 2006.

Paxton D.M., and B.J.Makenas, "Postirradiation Examination Report for the SP-3RR Test, WHC-SP-1053, 1993.

*Selection of Power Plant Elements for Future Reactor Space Electric Power Systems* Los Alamos National Laboratory, LA-7858, 1979.

Staff of the Solar Dynamic Power Systems Branch, *Solar Dynamic Power System Development for Space Station Freedom*, NASA/RP-1310, July 1993.

*Summary of Design and Analysis of the SNAP-50/SPUR Reactor Coolant Pump*. PWAC-467. August 10, 1965.

Tagawa, H., *Phase Relations and Thermodynamic Properties of the Uranium Nitride System*, Journal of Nuclear Materials, pp. 78-79, Vol. 51, 1974.

Touloukian, Y. S., et al, *Vol. 1 Thermal Conductivity Metallic Elements and Alloys*, Thermophysical Properties Research Center, Purdue University. IFI/Plenum, New York, 1970.

Touloukian, Y. S., et al, *Vol. 12 Thermal Conductivity Metallic Elements and Alloys*, Thermophysical Properties Research Center, Purdue University. IFI/Plenum, New York, 1975.

Touloukian, Y. S., et al, *Thermophysical Properties of Matter V. 13.*, Thermophysical Properties Research Center, Purdue University. IFI/Plenum, New York, 1979. P. 1153.

*Nuclear Safety Criteria and Specifications for Space Nuclear Reactors*, Dept. of energy, Document OSNP-1, Rev. 0, Washington, D.C. Dated Aug 1982,

Watson, W., *Short Time Properties of Advanced Alloys Tested at CANEL.*, Pratt and Whitney Aircraft- CANEL., April 20, 1965.

X-5 Monte Carlo Team, *MCNP – A General Monte Carlo N-Particle Transport Code, Version 5.*, Los Alamos National Laboratory, LA-UR-03-1987, April 2003.

## Distribution

List external recipients names and addresses

1	MS0736	John Kelly	6870
1	MS0736	Ronald J. Lipinski	6872
4	MS1136	Curtis D. Peters	6872
3	MS1136	Paul Pickard	6872
1	MS1146	Steven A. Wright	6872
1	MS1146	Roger X. Lenard	6872
2	MS9018	Central Technical Files	8944
2	MS0899	Technical Library	4536

For LDRD reports, add:

1	MS0123	D. Chavez, LDRD Office	1011
---	--------	------------------------	------

For CRADA reports add:

1	MS0115	CRADA Administration	10112
---	--------	----------------------	-------



**Sandia National Laboratories**